

TOPICAL REVIEW • OPEN ACCESS

Infrared imaging of photovoltaic modules: a review of the state of the art and future challenges facing gigawatt photovoltaic power stations

To cite this article: Claudia Buerhop *et al* 2022 *Prog. Energy* 4 042010

View the [article online](#) for updates and enhancements.

You may also like

- [Star Formation In Nearby Clouds \(SFINCs\): X-Ray and Infrared Source Catalogs and Membership](#)
Konstantin V. Getman, Patrick S. Broos, Michael A. Kuhn et al.
- [Anomalous contra-lateral radiometric asymmetry in the diabetic patient](#)
Edgar Israel Fuentes-Oliver, Crescencio García-Segundo, Rebeca Solalinde-Vargas et al.
- [Accurate OH Maser Positions from the SPLASH Survey. III. The Final 96 deg²](#)
Hai-Hua Qiao, Shari L. Breen, José F. Gómez et al.



TOPICAL REVIEW

OPEN ACCESS


RECEIVED
10 March 2022REVISED
24 June 2022ACCEPTED FOR PUBLICATION
11 August 2022PUBLISHED
14 September 2022

Original content from this work may be used under the terms of the [Creative Commons Attribution 4.0 licence](#).

Any further distribution of this work must maintain attribution to the author(s) and the title of the work, journal citation and DOI.



Infrared imaging of photovoltaic modules: a review of the state of the art and future challenges facing gigawatt photovoltaic power stations

Claudia Buerhop^{1,*} , Lukas Bommers¹, Jan Schlipf², Tobias Pickel¹, Andreas Fladung² and Ian Marius Peters¹

¹ High Throughput Methods in Photovoltaics, Forschungszentrum Jülich GmbH, Helmholtz Institute Erlangen-Nürnberg for Renewable Energy (HI ERN), Immerwahrstraße 2, 91058 Erlangen, Germany

² Aerial PV Inspection GmbH, Im Johannistal 31a, 52064 Aachen, Germany

* Author to whom any correspondence should be addressed.

E-mail: c.buerhop-lutz@fz-juelich.de

Keywords: IR-imaging, high throughput, relevance, image acquisition, processing and assessment

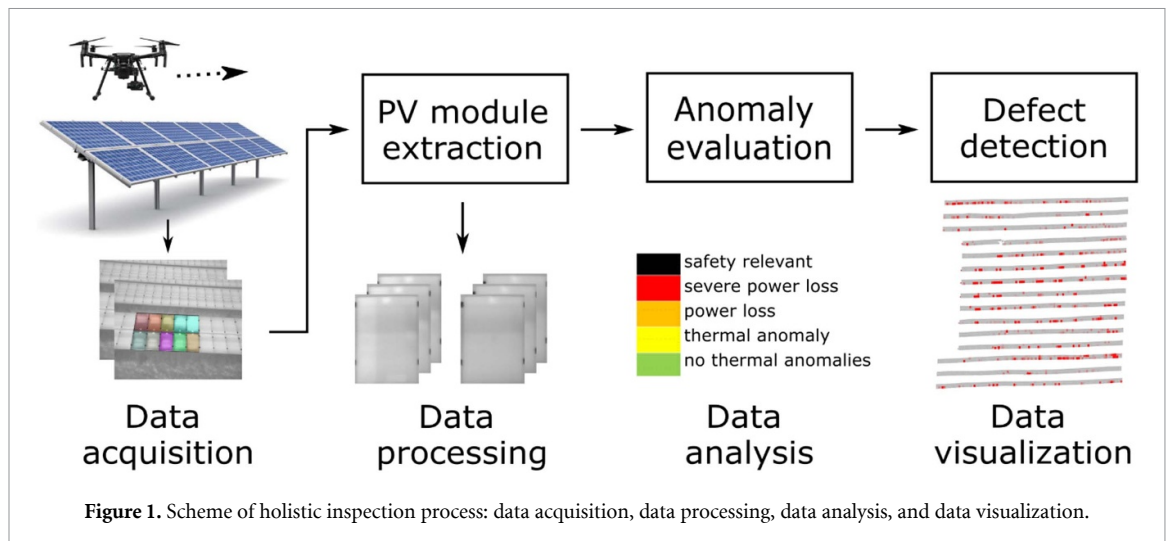
Abstract

Thermography is a frequently used and appreciated method to detect underperforming Photovoltaic modules in solar power stations. With the review, we give insights on two aspects: (a) are the developed measurement strategies highly efficient (about 1 module s⁻¹) to derive timely answers from the images for operators of multi-Mega Warr peak power stations, and (b) do Photovoltaic stakeholders get answers on the relevance of thermal anomalies for further decisions. Following these questions, the influence of measurement conditions, image and data collection, image evaluation as well as image assessment are discussed. From the literature it is clear that automated image acquisition with manned and unmanned aircrafts allow to capture more than 1 module s⁻¹. This makes it possible to achieve almost identical measurement conditions for the modules; however, it is documented to what extent the increase in speed is achieved at the expense of image resolution. Many image processing tools based on machine learning (ML) have been developed and show the potential for analysis of infrared (IR) images and defect classification. There are different approaches to evaluating IR anomalies in terms of impact on performance, yield or degradation, of individual modules or modules in a string configuration. It is clear that the problem is very complex and multi-layered. On the one hand, information on the electrical interconnection is necessary, and on the other hand, there is a lack of sufficient and suitable data sets to adapt existing computer vision tools to Photovoltaics. This is where we see the greatest need for action and further development to increase the expressiveness of IR images for PV stakeholder. We conclude with recommendations to improve the outcome of IR-images and encourage the generation of suitable public data sets of IR-footage for the development of ML tools.

1. Introduction

Thermography, also called infrared (IR) imaging, has been a frequently used tool for years to detect faulty or underperforming modules and strings in PV power plants. IR is so attractive because the images are taken during operation in a non-contact and non-destructive way without interfering with the electrical system. With this review, we address the question in how far today's methodology of thermography inspection meets the current and future requirements of researchers and industry. Two aspects are in focus:

- (a) Worldwide, the PV installation market is expected to grow annually by 200 GWp and more over the next five years [1] PV systems will be installed on water (floating PV), on facades (Building Integrated Photovoltaics), in agricultural environments (agri PV), and of course on large open spaces at Giga Watt

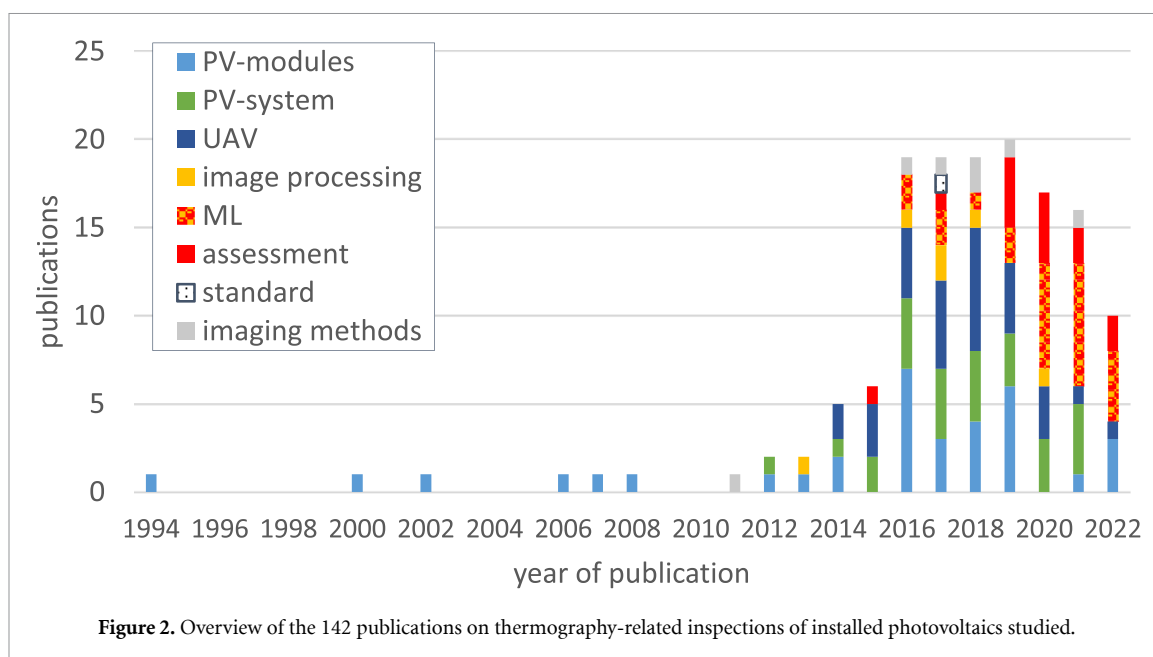


peak (GWp) scale. Important to power production will be ground-mounted, large and extended utility-scale multi Mega Watt peak (MWp) PV systems. We focus on these systems in the review. Let us do a small calculation example. Assume for simplicity a 100 MWp PV power station with 200 000 PV modules (each having 500 Wp) distributed over 300 hectares and e.g. 200 central inverters as well as changing micro climates throughout the installation site. With this review we want to paint a holistic picture of the inspection process: (1) data acquisition, (2) data processing, (3) data analysis, and (4) data visualization, as presented in figure 1. In continuation of the little example, assuming further that every second one module is inspected, and the recorded data is analyzed and evaluated, a total processing time of 7 d (each 8 h) would be needed to assess the entire plant. At 5 s of inspection process, it is in total 35 d of inspection time. While data acquisition is not the limiting factor to the inspection throughput, most time is spent, instead, on the data processing and analysis. All processing steps that require manual labor and cannot be automated in image analysis are time critical, as is training of models for data processing. Recent automated processing systems based on computer vision and machine learning (ML) have shown the potential to significantly reduce the time required for processing. However, for automated data analysis appropriate datasets and knowledge about failures need to be created: is a **time scheme of 1 s per module for analyzing GWp PV power stations** sufficient in order to locate underperforming modules and strings? We emphasize what is achievable with thermography according to the state of the art, but also possibilities for development potential.

- (b) Discussions with asset owners, EPCs and O&M companies reveal that they are aware of and appreciate the advantages of thermography. It enables fast and direct, non-contact, non-destructive identification and localization of malfunctioning or underperforming modules and strings without disrupting regular operation. ‘A picture is worth a thousand words’. Making faults visible by means of thermal anomalies can only be a first step, **statements about the relevance of the findings are lacking**, though for e.g. operation, service life, yield, or O&M. Can thermography provide the industry with this information to decide on necessary maintenance measures to secure operation and yield? We are therefore researching the literature for reliable, quantitative statements on performance reduction (power or yield) and/or degradation behavior of PV systems based on IR images.

The review shows what contribution thermography of state of the art makes to PV power plant inspection today, but also which developments can be beneficial to be prepared for future requirements, (a) fast and (b) expressive inspection tool. Scanning the publications of the current state of research and developments in industry and academia, PV-system-related thermography started already in 1994. As visualized in figure 2, we can distinguish four epochs in the development of IR thermography as a suitable tool for PV power plant inspection:

- (a) **IR**—in the first two decades IR-imaging started to move from the lab to outdoor application for PV module inspection as a fast and inexpensive tool. IR photographer walked through PV-systems and took IR-images of defective modules by hand. Defect signatures of real operating modules, such as substrings, potential induced degradation (PID), module strings, diodes, hot cells, solder defects, were collected.
- (b) **IR + UAV**—about 2014 first publications highlight the benefit of using drones or unmanned aerial vehicles (UAVs) as carriers for IR-cameras. The use of drones accelerated and facilitated the inspection



- process and laid the foundation for the automation of image acquisition. In 2017 Andrews [2] reports IR-inspections of PV-power stations by aircraft.
- (c) **IR + UAV + ML**—due to the immense image volumes, manual evaluation became too tedious and was increasingly replaced by automated image analysis since 2016. Now the images are digitized in order to be used for ML methods.
 - (d) **IR + EVAL**—since around 2018, we have seen the first efforts to evaluate (EVAL) and quantify the thermal anomalies found.

Since the first studies [3–5] on visualizing defects in PV modules under operating conditions, the interest and acceptance of thermography for quality control of PV modules and PV power stations has increased significantly. The focus was on the recognition, documentation and explanation of typical failure patterns of PV-modules in the IR images (marked in figure 2 as ‘PV modules’) and other established imaging methods such as electroluminescence (EL). Since the occurrence and relevance of defective PV modules can only be understood in the context of the PV system, this aspect is captured with the key word ‘PV system’ in figure 2. The success story of thermographic quality testing continued with the availability and usability of drones for civil applications, marked in figure 2 as ‘UAV’. In one fell swoop, the IR cameras on drones made it so easy to record large quantities of images of many PV modules in large PV power stations that it was no longer possible or practical to process the data manually. Available computer vision tools enhanced the research on algorithms for automated image processing and anomaly detection. Fault detection and classification can now be done using various ML methods. Successful fault/anomaly detection is important, but also requires quantitative evaluation in terms of relevance and impact on the yield of the PV system. Publications on the evaluation are summarized in the category ‘assessment’. Furthermore, the comparison of IR-findings with other imaging techniques are of interest and are listed under the headline ‘imaging methods’, e.g. EL, true color red-green-blue (RGB) -images. Since 2017, there is an international standard for thermographic inspection of solar modules [6], which is addressed as ‘standard’.

There are many reviews in the IR PV-related literature that indicate community expectations for IR testing of PV power stations and the potential to be disclosed. The reviews, listed in table 1, cover a wide range of aspects. They provide insights in optics and camera specifications [9], specifications of robots and drones [9, 10, 13], imaging techniques [11, 12, 14, 18, 19], module failures and their patterns [7, 8, 15, 17, 19], image processing [17], and ML tools [16]. This review is about IR testing of the PV system, not the PV module. It extends beyond the individual PV module and considers the PV module as a part of the electrical system and in connection with the grid. The aspect of high throughput of the inspection of GWp PV power stations is emphasized on an equal footing with the claim to state the relevance of the thermal anomalies. Relevance means which defect must be taken seriously, which can be ignored. EL is an alternative imaging technique which can confirm defects. A possible assessment may be based on hazard potential, performance, yield, or degradation over time. IV measurements and monitoring data can help classify and evaluate

Table 1. Summary of IR- and PV-related reviews in the period 2012–2021.

| Main aspect/topic | Authors | Year | Citation |
|---|------------------------------------|------|----------|
| Failures, module degradation, list of typical errors | Spagnolo <i>et al</i> | 2012 | [7] |
| Failures, modules | Tsanakas <i>et al</i> | 2016 | [8] |
| General principles + cameras and drones and specifications | Gallardo <i>et al</i> | 2018 | [9] |
| Drones, UAS towards automated inspection procedures, thermal anomalies, 3d photogrammetry | Rakha and Gorodetsky | 2018 | [10] |
| Imaging techniques | Jahn <i>et al</i> , IEA report | 2018 | [11] |
| Fundamentals | Herraiz <i>et al</i> | 2020 | [12] |
| Drones and IR-images of PV-systems, fundamentals | Rahaman <i>et al</i> | 2020 | [13] |
| Condition monitoring, fundamentals of thermography | Kandeal <i>et al</i> | 2021 | [14] |
| Visual faults, faults, power-reducing affects, faults and methods, data analysis | Venkatesh and Sugumaran | 2021 | [15] |
| Deep learning for infrared imaging-based machine vision | He <i>et al</i> | 2021 | [16] |
| Image processing: surface defects—internal—external problems, damage identification of PV, pictures of failures | Afifah <i>et al</i> | 2021 | [17] |
| Field-suitable mobile test equipment for PV-plants | Herrmann <i>et al</i> , IEA report | 2021 | [18] |
| Fault diagnostics for utility-scale PV systems, calculation of electrical parameters, thermography, faults + classification | Navid <i>et al</i> | 2021 | [19] |

performance losses. Interesting is how current methods are equipped for future tasks, e.g. inspecting a GWp PV power stations in continuous operation within acceptable time frames and with expressive reports.

The review is structured as follows: (a) brief introduction into thermal anomalies, identified failures and IR findings and their relevance for safe plant operation or system performance, (b) measurement conditions for IR-snapshots, which are important for image analysis but rarely discussed and included (on one hand measurement conditions can assist in root cause analysis, on the other hand be constraints for comparable image analysis), (c) core section highlighting: first; image acquisition and its responsibility for image quality and inspection speed, second, image processing for PV module segmentation, failure extraction and classification, and third, image evaluation, interpretation and assessment for giving insights into the relevance of the findings, and (d) discussion provides an overview of the lessons-learned, the consequences and the resulting need for development, i.e. which pieces of the puzzle are still missing in order to test large-scale PV power plants quickly and reliably and to make statements on relevance of their findings.

2. Failure modes in IR-imaging

In the early years thermal anomalies in IR-images were classified according to the patterns typical for distinct physical signatures, e.g. substring failure (open circuit or short circuit), diodes, cell fracture, PID. Many exemplary images of such failures, especially for 60 and 72 cell PV modules, can be found in the literature [8, 11, 18, 20, 21]. The classification of the observed anomalies changed in line with the efforts to make the evaluation more automated. The physical root-cause analysis became a phenomenological classification of the observations. Typically, PV-module faults are classified into visual, electrical, and miscellaneous faults [15, 22, 23]. The widely used classification of IR-anomalies suggested in the International Energy Agency (IEA) report [24] is shown in table 2. Cell cracks are usually not detectable with IR due to lateral dissolution limited by blurring caused by heat diffusion, as impressively shown by Muehleisen *et al* [25] using the example of modules after a hailstorm, here the existence of cell cracks was verified by EL.

Thermography is the imaging method that can make more than PV-module defects visible. Many deficiencies/deviations from normal operation can be detected using IR-imaging, namely:

- PV module faults [27, 28], all kinds of thermal anomalies and temperature gradients.
- Operational issues, e.g. disconnected strings/arrays/inverters, curtailment [29, 30].

Table 2. Classification of thermal signatures of PV-module faults can be found in IEA report [24] originally from feasibility study [26] but modified and extended.

| Thermal signature category | Description | Reason |
|----------------------------|--------------------------------|---|
| A | Whole cell part | Shunted, delaminated or partially shaded cell |
| B | Part of hot cell | Cracked cell, disconnected interconnector, or faulty solder joints |
| C | Single hot point = hot spot | Cracked cell or damaged busbar/interconnector, or artifact |
| D | Uniformly hot substrings | Fully active bypass diode |
| E | Patchwork pattern of hot cells | Short-circuited diode/fractured front glass, shunted diode (with increased occurrence close to frame: indication for PID) |
| F | Hot junction box | Poor connection causing ohmic heating |

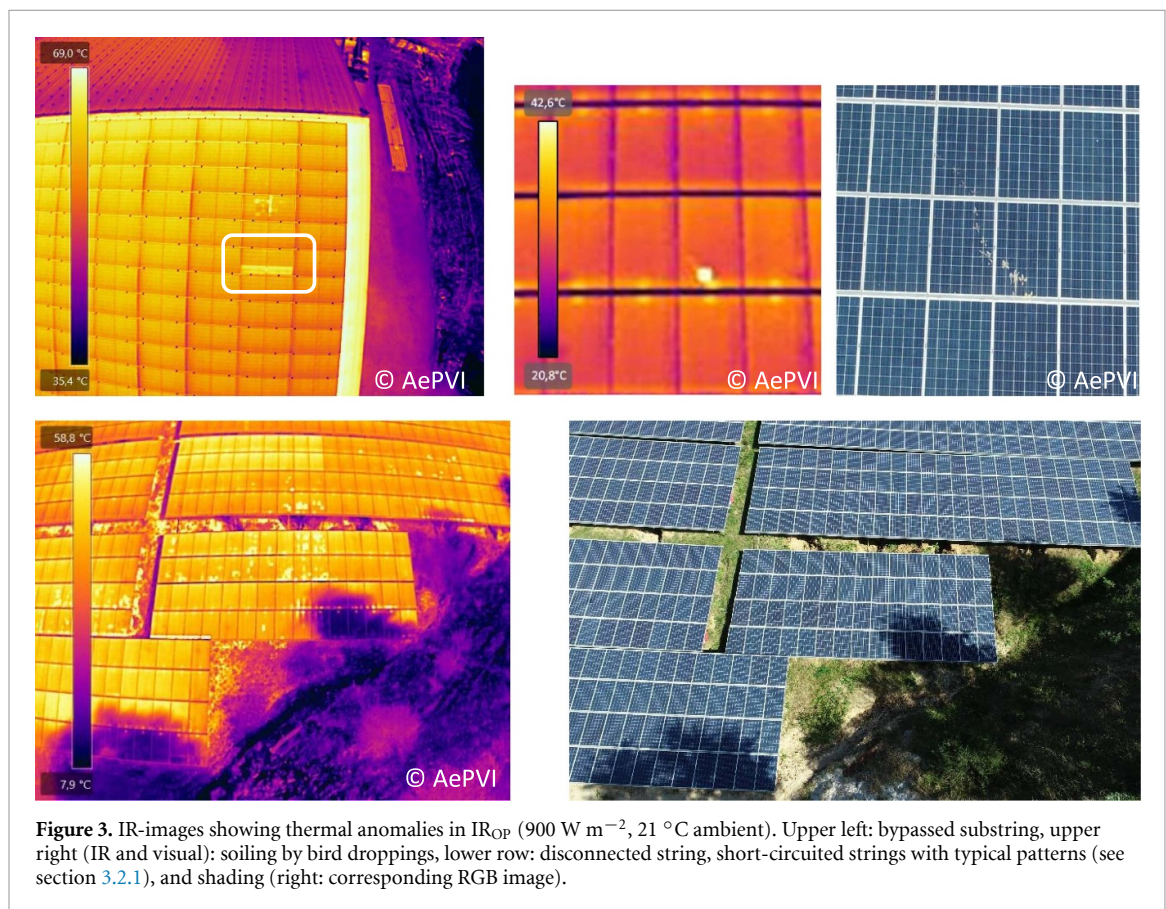


Figure 3. IR-images showing thermal anomalies in IR_{OP} (900 W m^{-2} , $21 \text{ }^\circ\text{C}$ ambient). Upper left: bypassed substring, upper right (IR and visual): soiling by bird droppings, lower row: disconnected string, short-circuited strings with typical patterns (see section 3.2.1), and shading (right: corresponding RGB image).

- External factors, e.g. soiling and dust [31], shading by stationary or changing/moving objects e.g. vegetation [30, 32], chimneys, high voltage lines [33], poles, partial shading [32].

Statistics from the years 2017 and 2019 show that PV-module and PV-array failures [29, 30] as well as shading [30] are frequently detected anomalies in IR-images. Especially during the commissioning period inactive tables, glass breakage, diode and junction box issues are the most frequent findings [34]. Examples of modules failures and external factors in IR images taken in normal operation mode (IR_{OP} , explanation below) are shown in figure 3.

Because of the limitations of one method to better understand observed findings, often supplementary and comparative measurements are carried out. For more details IR-images are enriched with EL images [35–38] or photoluminescence [39] or for power data with IV-measurements [40]. Frequently visual RGB-images are recorded simultaneously to the IR-footage in order to prevent misinterpretations due to artifacts, e.g. glass breakage, bird droppings, leaves, shading [41, 42]. An example for thermal anomalies due to soiling is given in figure 4.

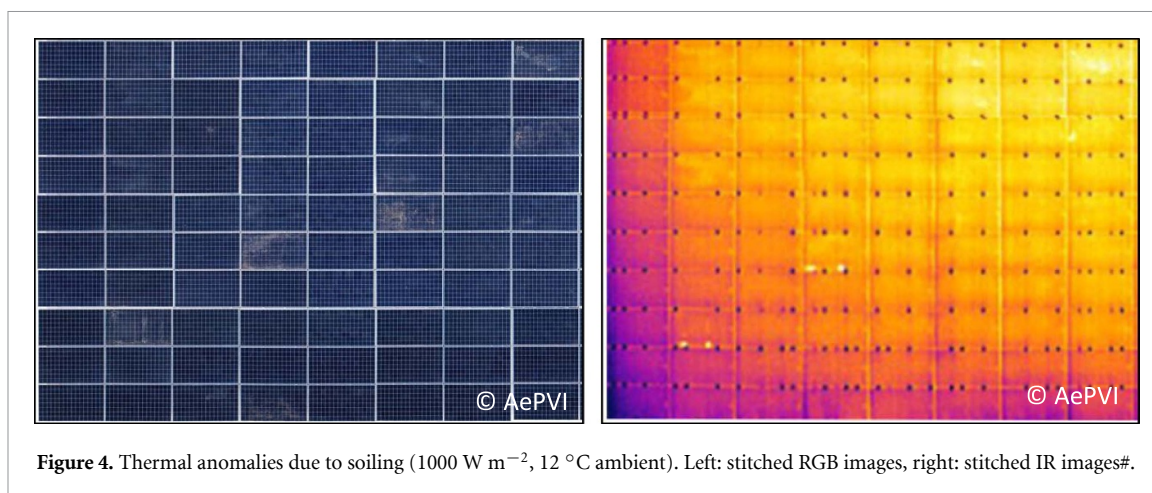


Figure 4. Thermal anomalies due to soiling (1000 W m^{-2} , $12 \text{ }^\circ\text{C}$ ambient). Left: stitched RGB images, right: stitched IR images#.

IR-imaging is also suitable to detect faults due to thermal anomalies in thin-film PV-modules [27, 43, 44] but will not be further discussed in this review. While thermography can be applied successfully to detect faults in all electrical equipment (e.g. inverters, combiner boxes, and cables) [27, 45] we will focus on its application to PV modules for the remainder of this article. Issues, that are easily detectable from the front side in PV-systems.

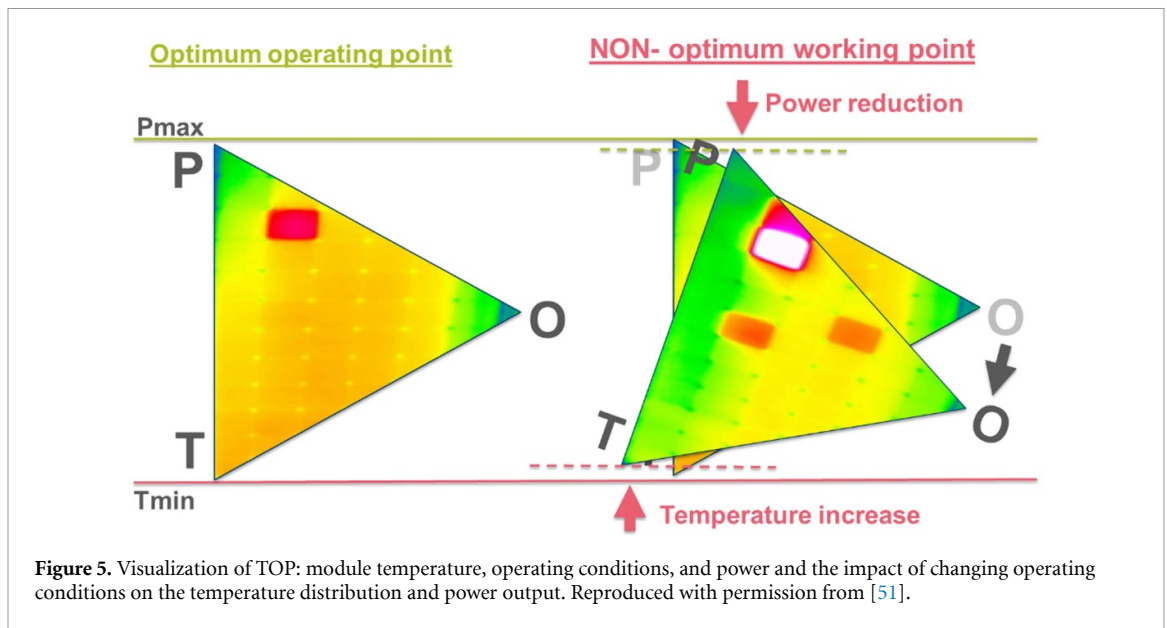
3. Measurement conditions

Measurement conditions provide the framework for high throughput and informative value of IR inspections. To achieve both, careful trade-offs must be made between the objectives. The dependence of IR images on the moment of external, given measurement conditions is outlined, first. Subsequently, the (additional) benefit of IR images at controlled operating conditions of the PV system for fault evaluation and root-cause analysis is presented. Here, a clear balance has to be made between additional benefits for error evaluation and fast and contact-free measurement performance.

3.1. Influencing factors

The measurement conditions are crucial for the recorded temperature distribution of the IR-snapshot and further analysis and assessment as well as for the time needed for the inspection including preparation. Thermography uses IR cameras to record heat radiation emitted by objects, in this case PV modules, in a non-contact and non-destructive manner. Global and local temperature differences or increases indicate faults and underperformance. For PV modules, solar energy that is not converted into electricity is converted into heat. Furthermore, low performing parts of modules can become consumers rather than producers of power and thus heat up considerably. Temperature increases are therefore a good indication of reduced performance and the presence of faults, but also a difficult task using the IR images. Aspects such as relevance and safety must be assessed using the absolute temperatures or temperature differences between anomaly and unaffected references. Even though temperature differences can be determined more reliably than absolute temperatures, temperature is still sensitive to changes.

The measurement conditions include all factors which influence the equilibrium between module temperature or defect temperature T and power P or power loss. These impact factors cover (a) electrical settings, e.g. strings length [46, 47], (b) operational configuration, e.g. maximum power point (MPP)-tracking or curtailment which define the operating point, (c) weather conditions, e.g. insolation E , temperature, wind speed, and (d) characteristics of a defective PV-module [48]. If one impact factor changes, the temperature-power balance of a defective PV-module changes, too [49–51], as visualized in figure 5. At operating point MPP the temperature is lowest and power output maximum. A shift of the operating point leads to increased power loss and increased temperature. The evaluation of the power loss of thermally conspicuous PV modules can be ambiguous: Module power at STC conditions or module power at field conditions or impact of defective PV module on string power in the field. The resulting numbers differ, following the example in [51], e.g. relative module power compared to nominal power: $P(\text{STC}) = 92\%$, $P(\text{field}) = 73\%$, and $P(\text{field} + \text{in-series with other modules}) = 58\%$. At that, knowledge of electrical configurations, string and inverter layouts (module optimizer, string inverter, or central inverters) are absolutely necessary.



However, the reaction time to changes, e.g. in weather conditions, is different for electrical current and voltage in comparison to temperature. The electrical parameters react instantaneously while the temperature adapts slowly [52, 53]. Patterns can change within minutes, e.g. the bypass diode becomes active, or throughout the course of the day (a short-circuited bypass diode/substring of a solar module shows a checkerboard-like thermal appearance in the early morning ($E = 400 \text{ W m}^{-2}$ and $T = 36 \text{ }^\circ\text{C}$) and one very hot cell in the substring in the early afternoon ($E = 900 \text{ W m}^{-2}$ and $T = 69 \text{ }^\circ\text{C}$)). Therefore, at least 15 min of unchanged weather conditions are widely recommended.

Another aspect that needs to be considered is moisture on the module surface. Dew is to be avoided at IR recordings because otherwise blurred IR-images are the result. Furthermore, the image quality is of importance. Camera properties, as wavelength, pixels, instantaneous field of view (IFOV) determine the limits of the lateral resolution, addressed in [6, 54, 55]. View angle and altitude/distance [55–57] also need to be taken into account. For inspections on cell level, altitude/distance as well as IR-sensors, lens data FOV/IFOV need to be adapted to measurement spot sizes of the cell technology to be analyzed, e.g. new half cells/modules.

3.2. IR methodology

IR-images capture and document thermal anomalies directly, instantaneously [58], and in real-time without operation interruption. For the preparation and subsequent evaluation of an IR inspection, geographical and mechanical site plans, electrical string plans, the inverter concept, grid influences (e.g. curtailment), module data and weather data must be examined in order to be able to explain any observed thermal anomalies during the inspection. Different IR measurement methods can be distinguished depending on the intervention in the PV array, e.g. [59]. We describe: IR-imaging in operation (IR_{OP} or IR_{MPP}), IR-imaging at short-circuit (IR_{SC}), IR-imaging at open-circuit (IR_{OC}), IR-imaging in inverse current (IR_{INV}), and IR-imaging rear-side (IR_{rs}). We will use a blue color scale for images of IR_{INV} to avoid confusion with IR_{SC} in green color scale and IR_{OP} , IR_{OC} in often used rainbow color scale. In the following, the procedures, advantages and limitations of the methods are presented. Classic IR drones can be used for all types of IR inspections. Technical modifications to the drones/IR-cameras are not necessary.

3.2.1. IR-imaging in operational mode (OP)— IR_{OP} or IR_{MPP}

The real operation conditions are recorded in the OP or at MPP. Since a PV array is not necessarily working in its MPP, the designation IR_{OP} is preferred over IR_{MPP} . Although an intervention in the electrical system is generally not necessary for IR_{OP} , knowledge of the operating conditions is beneficial. Therefore, electrical data of the sites monitoring system or own records provided by clamp ampere meters can be utilized.

IR_{OP} measurements [60] of PV power plants require minimum irradiances for the evaluation and generation of meaningful reports. In addition to the normative requirements of 600 W m^{-2} [6], measurements at lower irradiances are also possible, or even have a clearer significance, such as for PID at irradiances as low as 250 W m^{-2} [61]. Note: if normative minimum irradiation is required, the measuring times can turn out to be severely limited by seasonal fluctuations and location/country/continent.

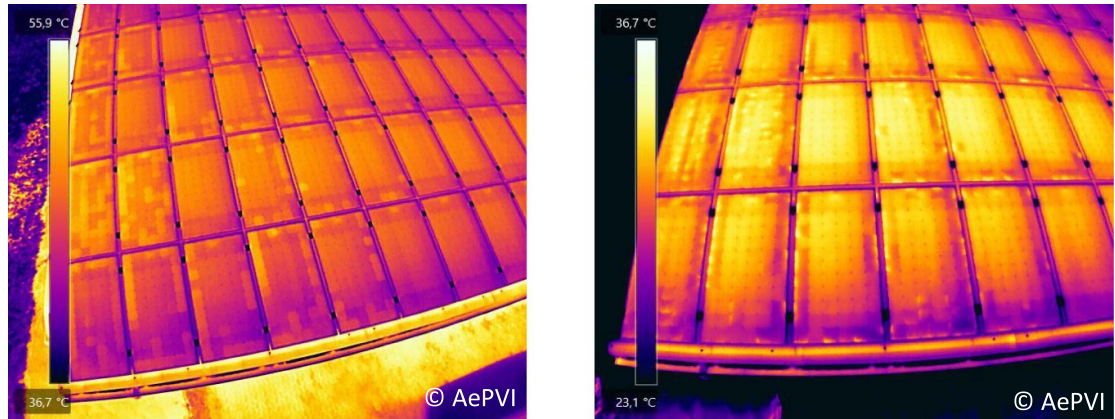


Figure 6. PID in IR_{OP} (left) and IR_{OC} (right) (700 W m^{-2} , $16 \text{ }^\circ\text{C}$ ambient).

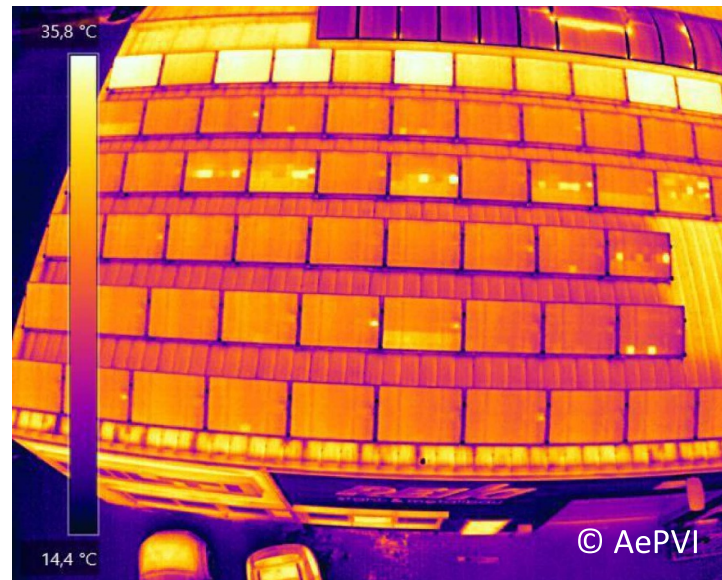


Figure 7. IR_{OP} (700 W m^{-2} , $23 \text{ }^\circ\text{C}$ ambient). In the uppermost string, five modules have been bridged manually. They are in idle mode (same temperature as the bypassed substrings visible in several other modules on the roof), but the remaining modules of the string are much hotter. The energy for that additional temperature increase originates from two other strings which are connected in parallel (not shown here).

3.2.2. IR-imaging at open circuit—IR_{OC}

For various types of faults, it can be very helpful to inspect the PV modules, not only in OP mode, but also in the open circuit mode (IR_{OC}). This is illustrated in figure 6 for the case of PID: in IR_{OP}, we find the typical pattern of hotter cells especially at the module borders. Additionally, we see in IR_{OC} that within these affected cells, the cell parts closest to the module frame are hottest. This underlines the diagnosis of PID where the notorious stray currents flow from the cell to the frame, thereby heating up the area. If the two operating conditions are compared directly with each other, some error backgrounds can be clearly identified, compare appearance of PID in OP and OC-mode in figure 6. For this purpose, the inverter must be disabled on the AC/DC side, all modules are then theoretically completely in open circuit. In the case of parallel-connected module strings with different module string voltages (due to shading/soiling/module faults), equalization currents can then already occur between them, which can be directly detected thermally. One or more strings then feed one or more other strings with lower voltages; these modules within the fed string appear significantly warmer than modules in no-load operation and indicate string/module problems. This is illustrated in figure 7. To avoid this phenomenon, all strings have to be disconnected from the inverter.

Likewise, the difference between IR_{OP} and IR_{OC} can clearly prove whether a bypass diode in a conspicuous substring is defective or was merely active. In addition, heavily loaded crystalline modules with PID can also be detected in the open circuit operating condition, see figure 6.

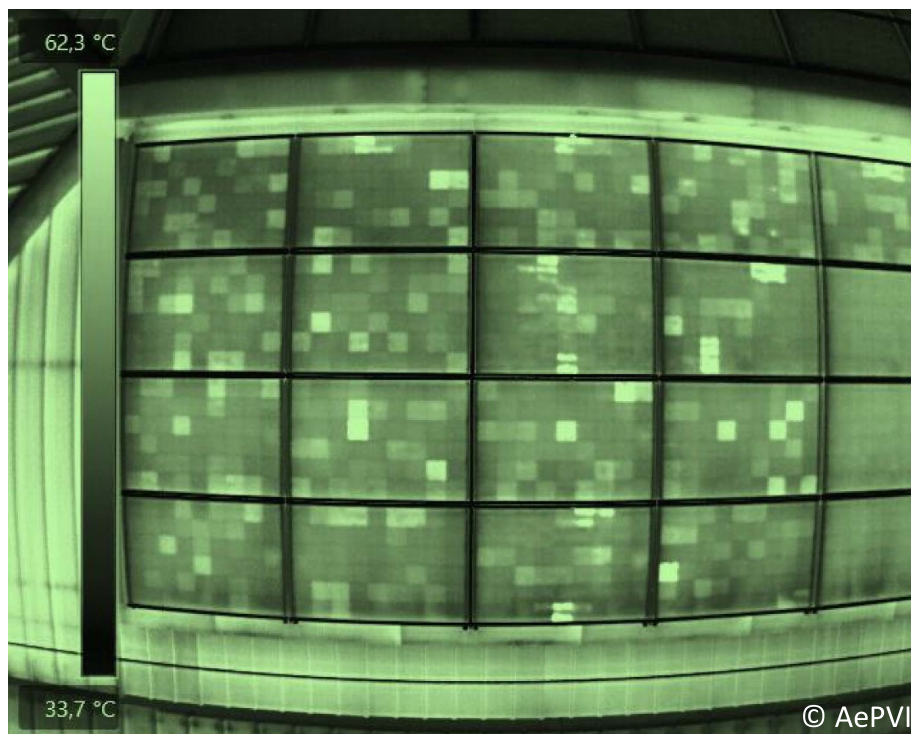


Figure 8. Patterns of cells in the short-circuited strings (IR_{SC} , 1200 W m^{-2} , $30 \text{ }^\circ\text{C}$ ambient).

3.2.3. IR-imaging at short-circuit— IR_{SC}

Measuring IR in short circuit (IR_{SC}) requires intervention in the DC electrical system and is therefore reserved for qualified and authorized electricians. For this purpose, the individual module strings are short-circuited by means of a suitable DC switch when solar irradiation $>150 \text{ W m}^{-2}$. Stronger crystalline cells in the short-circuited module/string start producing electricity immediately after the short-circuit; shaded, soiled, damaged cells with a weaker current in the module/string become consumers in the series connection and convert the energy produced by the stronger cells into heat. The usually chessboard-like thermal patterns that form, can provide information on cell mismatching (factory problem) as well as existing cell damage/shading or soiling already in the initial phase of the short circuit, see figure 8. Note that in this operating condition, the current flow I_{SC} in the substrings is higher than I_{MPP} . We use a green color scale here for IR_{SC} to avoid confusion with IR_{OP} or IR_{OC} .

This effect can be helpful with lower irradiances, on the other hand, cell problems basically become more obvious and are detected more easily. Post documentation of roof/string plans in daylight can also be implemented very quickly.

3.2.4. IR-imaging with power supply— IR_{INV}

An alternative to using sun light as an excitation source for PV-modules is the application of an external power source, similar to EL but recording the infrared heat radiation. This method is called ‘IR inverse’ (IR_{INV}) to emphasize the inverted operation of the module when current is supplied to produce heat. These measurements require an intervention in the electrical DC system and is therefore reserved for qualified and authorized electricians. For this purpose, the individual module strings are energized with $0.1\text{--}1 \times I_{SC}$ (depending on the module/failure type) by means of suitable DC power supplies when there is little or no solar irradiation, i.e. also at dusk or at night.

Due to the current applied to the modules/strings, the defect areas in the modules usually heat up faster in the first few seconds than the rest of the cell material at ambient temperature. In contrast to IR_{OP} scans at module/cell temperatures of $>70 \text{ }^\circ\text{C}$, these scans produce defects in a $5 \text{ }^\circ\text{C}\text{--}15 \text{ }^\circ\text{C}$ warm module. Thus, they produce a higher relative ΔT and more distinct heat signatures, as known for pulsed or lock-in thermography [43].

Depending on the module/environment temperature, the modules/strings are only energized for several seconds to make the faults visible. Figure 9 illustrates a typical IR_{INV} -pattern.

IR_{INV} examinations can be carried out at low irradiation or at dawn/night. This greatly increases the possible measurement deployment times for IR drone inspections worldwide. Due to the IR inspection with



Figure 9. Equipment used for energizing the PV strings at a combiner box (left and center), IR_{INV} image recording of a PV module revealing cell breakage (right).

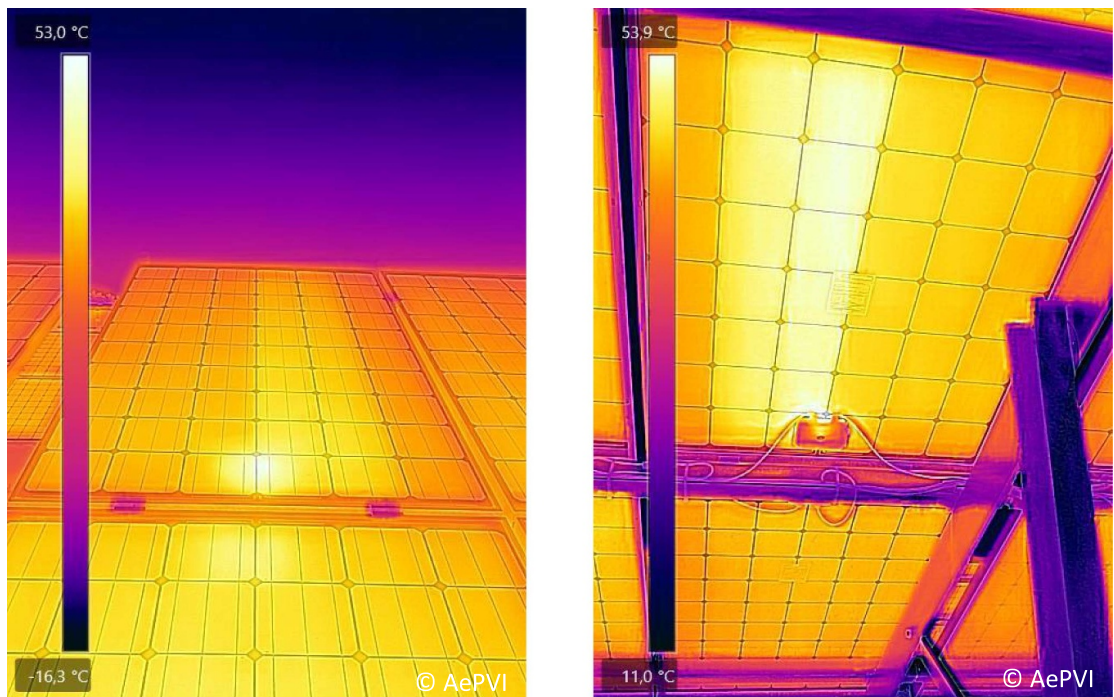


Figure 10. Front-side (left) and backside IR_{OP} (800 W m^{-2} , $25 \text{ }^\circ\text{C}$ ambient) displaying a substring failure. Note how the junction box is heating up due to the active bypass diode.

low/absent solar irradiation in the inverse procedure, shadowing and soiling of the solar modules no longer play a major role. Due to the lack of solar reflections compared to IR_{MPP} measurements, the (automated) detection of thermal anomalies is also much easier. Plants with different module orientations can therefore always be examined and evaluated under the same conditions, e.g. PV-modules orientated differently in an east–west-alignment. In contrast to IR_{MPP} measurements, the IR_{INV} method allows cell defects to be clearly detected. Cell breaks/cracks, high resistance cell connectors, busbar problems/current distributions, PID, etc can be detected down to the cell level.

3.2.5. IR rear side

IR-images from polymer rear side of the PV-modules can be beneficial (rear-side IR-imaging, see figure 10 for an example), because of different emissivity and thermal properties of front side glass and rear side polymer. The emissivity in the infrared spectral range for glass surfaces is $\varepsilon \approx 85\%$ [54, 62, 63] and for polymers $\varepsilon \approx 90\%–93\%$ [64, 65]. Furthermore, the blurring is reduced due to thin polymer layers behind the solar cell (ca. 0.5 mm) compared to the thick glass sheet in front of the cell (ca. 4 mm) by comparable low thermal diffusivity a of both materials (glass $a = 0.34 \text{ mm}^2 \text{ s}^{-1}$, polymer:polyethylen $a = 0.17 \text{ mm}^2 \text{ s}^{-1}$) [66]. For completion purpose, IR-images can also be recorded from the rear side of PV-modules as it was done for the extended All-Indian PV reliability survey 2016 [67] in order to study the electrical degradation of PV modules. The advantages are good access to PV-modules in open rack installations by high emissivity and therefore more reliable temperatures.

Because the emissivity of glass surface is $\varepsilon \approx 85\%$ in the infrared spectral range [54, 62, 63], IR-images from the highly emitting polymer rear side of the PV-modules can be beneficial (rear-side IR-imaging, see figure 10 for an example).

4. IR-image analysis

We analyzed literature about IR analysis of PV power stations to answer the questions: (a) is IR inspection fast enough to detect all relevant failures in GWp PV power stations, and (b) does IR imaging provide the information plant stakeholders, e.g. operators, are looking for.

4.1. Data acquisition—IR-image recording

To better and more efficiently exploit IR imaging of PV power stations, the recording technology has changed over time. Automated, enduring mobile robots and vehicles have largely replaced stationary systems (e.g. lifting platforms, cranes) and IR photographers (human labor). While ground-based measurements are still in use for certain scenarios and experienced IR photographers can manage up to 30 MWp a day (here only IR-images of suspicious PV modules are documented), airborne measurements are in general more common. When performing ground based measurements tripods and small motorized all-terrain vehicles, commonly known as quads, might be valuable tools to increase the operating range of the photographer. However, most often an airborne vehicle is used to carry the IR-camera through the PV power stations in the right position for the IR-images [57, 68, 69]. Especially UAVs [13] also known as drones, like multicopters, which are affordable, are often used. They are easy to navigate and to transport. Compared to ground-based measurements, airborne measurements have the advantage that hard-to-reach PV systems (e.g. floating PV, pitched roofs, facades of BIPV [5], rooftop installations, tracked PV systems [70]) can be inspected without problems. Several works [71–74] propose solutions for automatic flight planning and execution. References [71–73] extract outlines of the PV plant rows from available satellite imagery of the site using classic computer vision algorithms, such as thresholding. Subsequently, an optimal flight path is computed and transferred to the drone as waypoint mission [71]. To achieve accurate tracking of each row during the scanning procedure [72–74], propose the use of a row-following controller, which steers the drone based on visual feedback.

Aerial inspections using unmanned drones as well as manned aircrafts can be easily automated, both in route planning and navigation. This increases the throughput respectively reduces the acquisition time compared to conventional, hand-held methods significantly, as shown by a selection of publicly accessible data in table 3. Using drones the inspection time is reduced [75, 76], the factors vary, e.g. 10–15-fold [13, 21] or 50-fold [77]. The figures of state of the art methods show that with drones and aircrafts, more than 1 module s^{-1} can be recorded. Unclear remains frequently the level of inspection, i.e. the image resolution is not stated/reported which determines the anomaly detection. Standard IEC TS 62446-3 Edition 1.0 2017-06 recommends at least 3 cm px^{-1} as ground sample distance. A systematic and automated image acquisition enables the automation of the subsequent image processing and evaluation/assessment, as will be shown below [78, 79].

IR-inspection of PV power stations using drones is fast, simple and inexpensive, stated by Spagnolo *et al* [7]. Weinreich highlights *fast* by 10–20 MWp per photographer and day [30]. The *costs* range between 1800 Euros to 2740 Euros a day, or 225 Euros MWp^{-1} , giving accurate results by a flight altitude of 15 m [80]. Confirmed by Weinreich *et al* [30] for plants larger than 100 kWp. Companies offering drone-based IR inspections are, e.g. *Above Surveying*, *Rapotormaps*, *Sitemark*, *AePVI*, *Volateq*, *PV Service Pro*.

For extended utility-scale PV power stations of several 10 MWp or 100 MWp, the use of manned aircrafts with high-resolution camera systems makes sense [2, 89]. Despite the large distance between the solar module and the camera system, cell defects such as PID can be detected. The big advantage is, that extended PV power stations can be inspected very fast, i.e. under approximately similar environmental conditions [2, 86, 90]. In summary, image acquisition does not appear to be the limiting step for inspection time, neglecting image resolution and defect detection.

All methods benefit from direct detection of the thermal anomalies during operation, i.e. IR_{OP} . However, further thermographic measurements can be very helpful to identify the root cause of an observed anomaly. In figure 11, measurements of IR_{OP} , IR_{OC} , IR_{SC} , and IR_{INV} are shown. By combination of the observations, the highlighted substring failure can be explained. Generally, three possible scenarios can lead to this phenomenon: (a) an active bypass diode, (b) a faulty bypass diode, (c) an electrical failure in the module substring. In IR_{SC} , we observe the typical checkerboard patterns that occur due to the performance differences of the PV cells: in the short-circuited string the better cells produce current which is turned into heat by the worse cells. However, the pattern is absent in the discussed substring, indicating no electrical connection. This is emphasized also by IR_{INV} , where the substring appears cooler. Note, that some module

Table 3. Overview of reported inspection information related to acquisition time of IR-images of some sources without claim to completeness.

| Measurement type | Capacity | Inspection time | Image resolution | Camera resolution | Flight speed | Comment | Data source | |
|------------------|--------------|-----------------|---------------------------|-----------------------|-----------------------|----------------------------|-------------|------|
| Hand-held | 1 MWp | 10 h | — | — | — | — | [76] | |
| | 4000 modules | 8 d | — | — | — | 1 module min ⁻¹ | [80] | |
| Unmanned drones | 1 MWp | 10 min | — | — | — | — | [81] | |
| | 1 MWp | 1 h | — | — | — | — | [82] | |
| | 1.3 MWp | 0.5 h | — | — | — | — | [83] | |
| | 2–3 MWp | 1 h | Depends | — | — | — | [11] | |
| | 3.2 MWp | 32 min | — | — | — | — | 2 rows | [84] |
| | | 18 min | — | — | — | — | 3 rows | |
| | 6–8 MWp | 3–4 h | — | — | 640 × 480 | — | — | [85] |
| | 10 MWp | 1 h | — | — | — | — | — | [76] |
| | 10 MWp | 1 d | — | 3 cm px ⁻¹ | — | — | — | [86] |
| | 40 MWp | 1 d | — | Low resol. | — | — | — | — |
| | 74 MWp | 24 h | — | — | — | — | — | [75] |
| | 30 Mwp | 6 h | — | — | — | — | — | — |
| | 21 MWp | 7 h | — | — | — | — | — | — |
| | 13 Mwp | 4 h | — | — | — | — | — | — |
| | 40 MWp | 1 d | — | — | 640 × 512 | — | — | [77] |
| — | — | — | 10–15 cm px ⁻¹ | — | 48 km h ⁻¹ | Overview, string-level | [87] | |
| — | — | — | 5–6 cm px ⁻¹ | — | — | Module-level | — | |
| — | — | — | 3 cm px ⁻¹ | — | — | Abs. temp. | — | |
| — | — | — | 3 cm px ⁻¹ | — | — | Hot spot detection | [55] | |
| Manned aircrafts | 4000 modules | 5 min | — | — | — | — | [80] | |
| | 100 MWp | 1 h | — | — | — | — | [86] | |
| | 300 MWp | 1 d | — | — | — | 200 MWp in 1 flight | [88] | |

types do not show these patterns in IR_{SC} at all, possibly due to excellent matching of cells with the same performance. In figure 11, we find no checkerboard pattern in the substring in IR_{OP}. We can conclude that it is case (c), an electrical failure in the substring. If it had to do with the bypass diodes, the pattern would be present in IR_{OP}, too, and IR_{OC} would finally tell us if the bypass is merely active (no pattern) or defect (pattern visible). Experience shows that most substring failures found in the field are due to electrical failures in the module (not the bypass diodes).

Instead of an intervention into the system, as necessary for IR_{OC}, IR_{SC}, IR_{INV}, or IR_{backside}, often another IR_{OP} measurement at a different irradiance is a useful alternative.

In the end, the no-fly zone determines the technical specification of the sensor platform: aircraft for extended open space PV power station, drone for roof, facade, floating, open space PV power stations, alternatively, quad for open space PV power station, lift/high tripod for facade and pitched roof, and handheld/steady camera for flat roof PV systems.

4.2. Data processing—IR-image segmentation, classification

4.2.1. Detection of PV-modules in IR-videos

Many existing works utilize classic image processing techniques for the detection of PV modules in IR videos. A popular technique is (adaptive) binary thresholding of image intensities—usually applied after other means of image pre-processing—to obtain segmentation masks of PV modules [91–97]. Other methods detect PV module edges with morphological operations (opening, closing) [98, 99], the Canny edge detection algorithm [100, 101] or the Hough transform [100, 102]. Another technique for PV module detection is template matching [103]. Here, a template image of a PV module is moved over the input image in a sliding window fashion, a correlation metric is computed at each position, and the maxima are selected as potential location of PV modules. Jeong *et al* find candidate PV module regions (rectangular boxes) with the maximally stable extremal regions (MSERs) algorithm and filter out over-/undersized candidate boxes [104].

Disadvantages of these classic image processing techniques is their reliance on manual priors and heuristics, their need for extensive manual hyper parameter tuning, and most importantly poor generalization to unseen imagery.

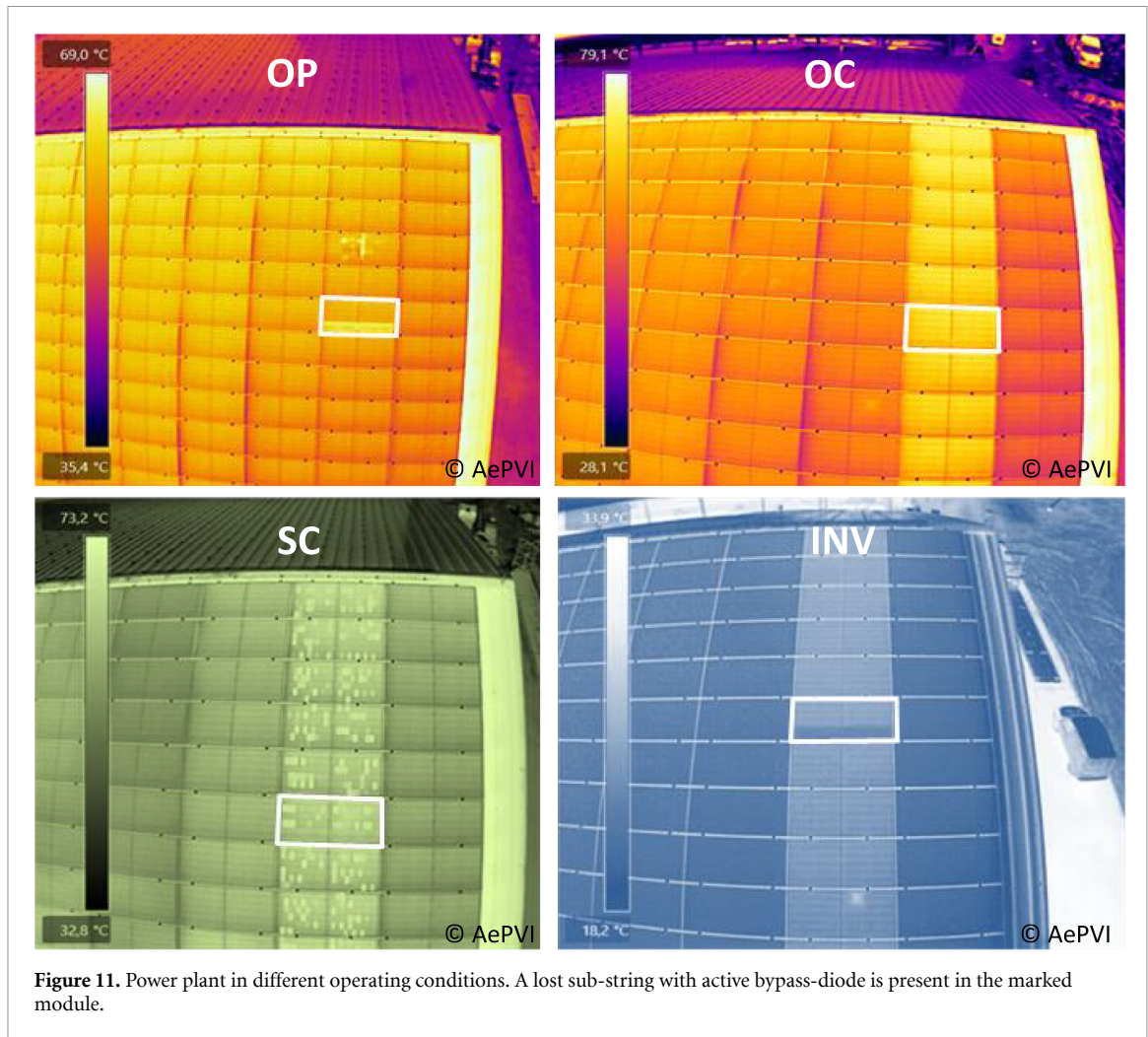


Figure 11. Power plant in different operating conditions. A lost sub-string with active bypass-diode is present in the marked module.

To overcome these issues, deep learning has been employed recently for PV module detection in IR images. Zhang *et al* perform semantic segmentation by means of a U-Net architecture with ResNet-34 backbone [105]. This approach distinguishes PV modules from the image background, however, does not differentiate between individual PV modules. The YOLOv3 object detector used by Greco *et al* distinguishes individual PV modules, however, provides only the bounding box of each module instead of a pixel-accurate mask [106]. Bommers *et al* and Vega Díaz *et al* use the Mask region-based convolutional neural network (R-CNN) instance segmentation framework to overcome both problems and obtain a pixel-accurate segmentation mask for each individual PV module [107, 108]. Furthermore, Vega Díaz *et al* find Mask R-CNN to outperform a baseline algorithm, which obtains PV module candidate regions with adaptive thresholding and classifies extracted texture features with a support vector machine. Table 4 summarizes the related works in terms of their methods and size of their datasets used. The analysis of dataset sizes reveals that many works use very small datasets, which raises doubts about the general applicability of the developed methods. Especially in the context of deep learning, training on small and low-variance datasets causes model overfitting, which hampers generalization.

4.2.2. Detection of PV module anomalies

Similar to the PV module detection, many existing works identify anomalous PV modules in IR images with classic image processing techniques. The most popular one is binary thresholding of image intensities, which segments hot regions of PV modules corresponding to thermal anomalies [91, 92, 97, 102, 104, 109]. Other techniques are k-means clustering of pixel intensities [110], fuzzy rule-based classification [111], color image descriptors [112] and the iterative growth of segmentation masks starting from local intensity maxima [100, 113]. Addabbo *et al* propose template matching for the localization of hot regions [103].

Due to their reliance on classic image processing all these techniques require extensive manual hyper parameter tuning and do not generalize well to unseen imagery. Furthermore, these works only detect the

Table 4. Literature overview of methods for PV module detection and anomaly detection. Traditional ML and deep learning methods are highlighted in italic and bold, respectively. All other methods use classic image processing. Datasets of sufficient size (in our opinion) are highlighted in bold.

| Source | Dataset size (images/modules/plants) | PV module detection | Anomaly detection |
|--------------|---|--|--|
| [91, 92, 94] | 34/—/1 | Binary thresholding | Binary thresholding |
| [93] | 37/1 554/1 | Binary thresholding | <i>Manual feature extraction + Grubb's test/Dixon's Q test</i> |
| [95, 96] | 3/204/1 | Binary thresholding | — |
| [97] | 120/—/1 | Binary thresholding | Binary thresholding |
| [98, 99] | n.a. | Morphological operations | — |
| [100] | 14 215/14 215/>1 | Canny edges + Hough trans. | Iterative growth of segmentation mask |
| [101] | 4/4/1 | Canny edge detection | — |
| [102] | 1171/84/>1 | Hough transform | Binary thresholding |
| [104] | 40/240/1 | Maximally stable extremal regions (MSERs) | Binary thresholding |
| [103] | 270/—/1 | <i>Template matching</i> | <i>Template matching</i> |
| [105] | 235/—/1 | U-Net semantic segmentation | — |
| [106] | 50 499/—/>1 | YOLOv3 object detection | — |
| [107] | 100/—/3 | Mask R-CNN instance seg. | — |
| [108] | 453 511/11 644/7 | Mask R-CNN instance seg. | Supervised classification with CNN |
| [109] | <10/3/1 | — | Binary thresholding |
| [110] | 4/4/1 | — | <i>k-means clustering of pixel intensities</i> |
| [111] | 120/120/1 | — | <i>Fuzzy rule-based classification</i> |
| [112] | 315/315/1 | — | <i>Color image descriptors</i> |
| [113] | <10/2/1 | — | Iterative growth of segmentation mask |
| [114] | 375/375/1 | — | <i>HoG features + naïve Bayes classifier</i> |
| [79] | <10/—/1 | — | VGG-16 semantic segmentation |
| [115] | 9000/9000/6 | — | Faster R-CNN object detection |
| [116] | 783/783/1 | — | Supervised classification with CNN |
| [117] | 1000/1000/>1 | — | Supervised classification with CNN |
| [118] | n.a. | — | Supervised classification with CNN |
| [60] | 93 220/93 220/28 | — | Supervised classification with CNN |
| [119] | 1428/480/1 | — | R-CNN object detection |
| [120] | 4160 000/105 546/6 | — | Domain-agnostic CNN + k-nearest neighbor classifier |

presence of relatively large and connected hot spots with large local temperature gradients. That makes them prone to miss important types of anomalies, such as PID.

Again, machine learning and deep learning have been used recently, to overcome these problems. For example, Oliveira *et al* [79] use a segmentation model based on the VGG-16 CNN to segment three different module anomalies directly in the IR video frame. Vlaminck *et al* [115] also operate directly on the video frame and employ a Faster R-CNN object detector to obtain bounding boxes of PV modules that contain a thermal anomaly. Opposed to that, other methods operate on images of individual PV modules instead of the entire video frame. For example, Dotenco *et al* extract hand-crafted features, such as mean and standard deviation, for each PV module and identifies outlier modules by means of a cascaded Grubb's test and Dixon's Q test [93]. Similarly, Niazi *et al* extract histogram of oriented gradients (HOGs) features and classify them using a naïve Bayes classifier [114]. Dunderdale *et al* extract scale-invariant feature transform (SIFT) features and apply a supervised random forest classifier to distinguish between four different types of module anomalies [116]. The same work finds a MobileNet and a VGG-16 CNN outperform the random forest classifier for classification of anomalous modules. The works by Manno *et al* [117], Zefri *et al* [60] and Ramirez *et al* [118] follow the same line of research. Similarly, Bommès *et al* train a ResNet-50 CNN for the classification of ten different modules anomalies [108]. Their dataset comprises of 450 000 images and is significantly larger than the datasets used in other works (see table 4). Bommès *et al* also demonstrate that collecting multiple images for each PV module benefits classification accuracy. By using the R-CNN object detector Su *et al* [119] predict not only the type of module anomaly, but also obtain bounding boxes, which localize the anomaly within the module image.

While these early adoptions of deep learning methods achieve high accuracies on their respective test datasets, they do not consider the inevitable domain shift between training and test data distributions. This

problem was examined in a more recent work of Bommès *et al* [120]. As an initial solution to the domain shift problem, a k-nearest neighbor classifier operating on less domain-specific supervised contrastive representations, was proposed. However, this classifier only makes a binary decision and cannot distinguish different types of anomalies. Thus, accurate classification of different types of PV module anomalies in IR images in the presence of domain shift between training and test data remains an open problem.

4.2.3. Spatial localization of PV modules in a PV plant

Accurate localization of PV modules in a large-scale plant based on an aerial IR video is an important task as it facilitates targeted repairs of defective modules. However, it is also a difficult problem as the video is highly repetitive and shows only a small local viewport with only a few PV modules at a time.

As a partial solution to the problem, Henry *et al* mark the global positioning system (GPS) position of the drone on a map whenever a video frame contains an anomalous PV module [71]. While being simple this approach only obtains an approximate position of the anomalous module.

A few works solve the localization problem by stitching subsequent video frames into a panorama image of an entire PV plant row [91, 92, 98]. This was shown to work well for short video sequences but localizes modules only relative to another. To provide the location in absolute reference frame, Niccolai *et al* extend the method by matching each row panorama to a computer-aided-design (CAD) plan of the plant by means of the GPS coordinates of the panorama center points [94]. Problematic is the need for a standardized CAD plan, which is not always available.

A different approach is the creation of an orthophoto of the entire PV plant from a high altitude [41, 121, 122]. This requires nadir images with a suitable overlap which may not always be feasible in case of nearby power lines, streets, or train tracks. Most importantly, the spatial resolution of a high-altitude image is low making fine-grained anomaly classification of PV modules difficult.

Several works propose direct georeferencing to obtain geocoordinates of each pixel in each video frame [103, 123]. While this is an elegant approach it requires nadir images and highly accurate GPS position estimates that can only be achieved by real-time kinematics GPS. The approach does not consider visual cues but relies only on GPS measurements, making it prone to GPS measurement errors.

Bommès *et al* [84] and Zefri *et al* [60] propose a more robust method for direct georeferencing that uses both GPS measurements and visual cues [84]. The method used structure from motion to reconstruct the camera trajectory and to obtain accurate geocoordinates for the corners of each PV module.

4.3. Data assessment—IR-image evaluation, relevance for system performance

Besides anomaly detection and defect location, evaluation and assessment of the IR-findings is of importance and interest. The aim is to link performance/yield/power loss with detected changes in the temperature distribution or fault-specific IR patterns and resulting recommended actions for O&M. Increasing temperature means reduction in power and vice versa. But there are many influencing factors that make the quantification of the power loss under real operating conditions challenging. The most important factors are, e.g. changing (temporal and local) weather conditions, unknown operating point (ideally MPP), unavoidable (and mostly unknown) external influences from the grid (e.g. curtailment), operating of PV-modules in serial and/or parallel electrical connection, IV-characteristic of each solar cell [124]. An interesting more fundamental approach is presented by Catalano [125], a power balance model is used to estimate the generated (dissipated) power for the individual cells, which has an error less than 1% for shunted cells.

Especially when linking IR-findings to yield losses it is utterly important that mentioned factors and other power relevant faults might affect a PV-power station, but not necessarily during an IR-inspection. Figure 12 shows an example for the electrical performance of a PV-power station on a day where IR-measurements took place. While during the actual measurement the overall performance fulfilled the expectations of the IR-findings, before and after the measurement parts of the plant were affected by shading and an inverter fault, which caused the outage of some PV-strings.

There are several approaches to correlate the module temperature with the module power [126] and degradation [67, 127]. Vergura and Marino [128] classifies the efficiencies by a framework analyzing the cells and clusters of cells: $\Delta T \approx 10$ K provokes 4% efficiency reduction, $\Delta T \approx 18$ K causes 7%–10% efficiency decrease. Teubner [129, 130] calculates the relative power reduction of a PV module based on its average module temperature in relation to that of an open-circuited reference module. The remaining power of PID-affected modules correlates well with the number of heated cells [131–133]. Verifying the derived/deduced power of a defective PV-module from its IR-signature can be done by either IV-measurements or monitoring on module level. In utility-scale projects without string monitoring thermography scans are becoming more important to locate the weakest modules in the string and to prioritize corrective maintenance [134]. Module level monitoring data verify voltage drops [51, 135] for defective modules with increased temperatures due to the shift of the working point. Moreton *et al* [136]

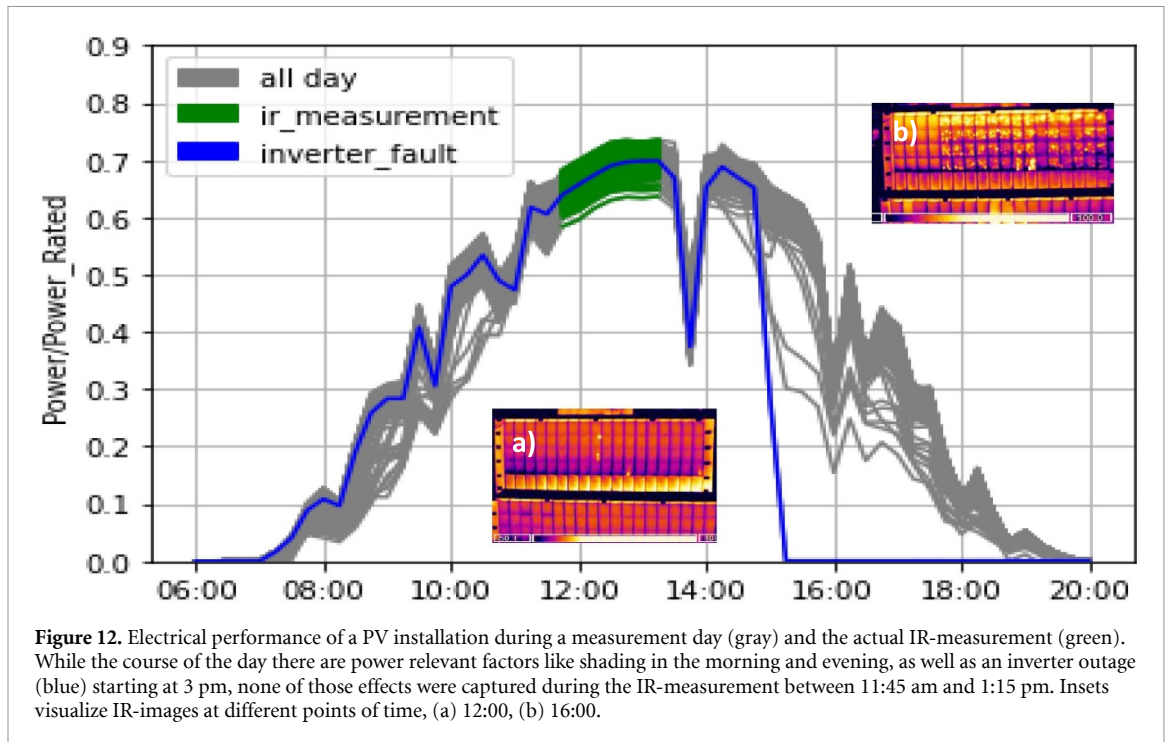


Figure 12. Electrical performance of a PV installation during a measurement day (gray) and the actual IR-measurement (green). While the course of the day there are power relevant factors like shading in the morning and evening, as well as an inverter outage (blue) starting at 3 pm, none of those effects were captured during the IR-measurement between 11:45 am and 1:15 pm. Insets visualize IR-images at different points of time, (a) 12:00, (b) 16:00.

studied explicitly the correlation between temperature difference and voltage drop and showed the impact of MPP-tracking on the operation point and on the temperature difference, which fluctuated strongly for low irradiances. Heated cells, namely hot spots, are studied and modeled in order to prevent failures [136–140]. Islam *et al* [141] describes a linear performance loss for defective PV-modules with increasing temperature difference between heated defect and the ambient temperature. Muttillio *et al* [142] extracted failure characteristic electric values (MPP, I_{SC} and V_{OC}) from defective PV-modules in correlation with IR-images of a test-string. Pinceti *et al* [143] presented a mathematical model to correlate temperature increase with power loss and economical income reduction. Using data from module optimizers [144] or IV-measurements [136] can also support power prediction but first, do not reflect real operating conditions of the majority of PV modules in the open space installation and second, provide data for the single PV module at certain ambient conditions. An extended degradation study of thermal anomalies of 53.5 GWp by aircrafts reveals that the fault degradation progresses faster in higher temperature zones and with site age, shown for unattributed hot spots and warrantable defects [127].

More important than the exact assessment of the power degradation of an individual defective PV module is the impact on the system performance to which the module belongs. Because of the difficulties to transfer the data from single modules to modules in a string configuration and to determine the impact on the string/array (e.g. double strings i.e. two strings in parallel) performance Dalsass *et al* [93, 145–147] and Skomedal *et al* [148–151] investigated monitored array data. Both combined IR-images with production data on string level. They analyzed/aggregated daily yield data of the month before and after the IR-inspection. They found/defined substrings, which are protected by diodes, as the smallest detectable unit. According to Dalsass and Skomedal, most important on string level is the number of module substrings containing thermal anomalies. The performance of a string with 60 substrings (20 modules each having three substrings) is on average reduced by $1.16 + 0.12\%$ per module substring containing thermal anomalies, which is less than expected ($1/60 = 1.6\%$). In addition, a shift of the operating point takes place according to Dalsass *et al* [152].

For a meaningful and quantitative analysis and evaluation, the irradiation data and module temperatures should be logged due to the thermal delay. For extended PV power stations several measurement units should be distributed throughout the PV power station, because the micro climate can differ significantly (due to shading, haze, fog, dust, stratosphere, cloud formation and so on).

Furthermore, the evaluation and quantification of defective module in the field is still difficult and unclear. There are no clear qualification criteria. Most authors rate the determined module power to standard test conditions (STC)-conditions. Moreton made suggestions for rejection and acceptance criteria. Suggestions to investigate the performance of defective PV-modules in the context of the PV-system are given by Dalsass and Skomedal.

5. Discussion

Lessons-learned from the literature show that much has been achieved in recent years, both for high-throughput IR inspections in GWp PV power stations and in terms of the relevance of the findings. Nevertheless, we have identified three pillars of development needs to provide value to stakeholders/users of such IR measurements in the future. We see unused potential in the area of data acquisition, image processing and image assessment.

First, **image acquisition** is the execution of the inspection. The use of aircraft and less expensive drones in combination with suitable camera systems has been further developed and expanded in recent years. While aircraft can inspect many MWp from a height within a short period of time, drones with lower flight altitude and thus better resolution require ten times longer. State of the art is that drones can inspect 1 module s^{-1} of multi MWp PV power stations. However, the reports do not provide insights into image quality, if the image resolution is sufficient for an expressive image assessment, that are useful for PV stakeholders. Furthermore, it is documented that extended drone-based missions are carried out within 1 d. The question of the influence of changing measurement conditions during the course of the measurement day on the evaluation and assessment remains unanswered. Promising is that drones are suitable for daytime operations. For the introductory example of a GWp PV power station a continuous drone-based IR inspection for at least 70 daytime operations is needed. This demands robust systems for permanent and ideally autarkic operation under harsh environmental conditions, where PV power stations are located. Solutions are necessary, adapting examples like the powered, controlled helicopter ‘ingenuity’ as part of the NASA Mars mission 2020 [153], or autonomous flying drones for medical purposes to remote islands [154], for PV. Parallelizing and coordinating the operation and communication of autonomous drones in swarms is also an alternative, but further developments and adjusted regulations are needed. Smart drone operation strategies can then control route planning and navigation.

Second, **image processing** has been the focus of research in recent years, and much has already been done on anomaly detection and failure classification. ML has become an important part of the processing techniques. The published metrics emphasize the quality of the developed tools, the relevance and benefit for the PV community is often unclear because type of failures and their quantities are not included. In general, there is a lack of suitable data sets with a sufficient number of examples of certain error patterns, a lack of relevance of the evaluated observations, e.g. bird droppings. As a consequence, many ML methods suffer from the limited certainty of a prediction.

In literature, the dominant successor technologies to 60 and 72 cell modules, e.g. half-cut/butterfly modules, do not yet play a role. Because of the special electrical connection of these modules, standard analysis tools may misinterpret the symmetric thermal anomalies, which are caused by a failure in only one half, see figure 13.

Here, the establishment of an IR image dataset with international participation can help to fill the gaps and promote algorithm development for all.

Third, **image assessment** aims to indicate the relevance of the observed anomaly for performance, yield and safety of the PV power thermography. The weakest modules in the string can be identified by their temperature rise. That these are not necessarily all defective modules as shown by comparison with EL records, see figure 14. To get clarity about the extent of defects and the impact of the defects, especially cell fractures, PV stakeholders should consider supplementary measurements, such as IR_{INV} , IV curves, EL, PL, see figure 15, depending on their objectives.

The limited number of publications on performance evaluation show that this is difficult. Many influencing factors must be known and should be taken into account. Basic knowledge must be built up, e.g. knowledge of electrical configurations and string/inverter layout (module optimizer, string inverter, or central inverters). The power loss of PV modules is not defined. Is it the power loss of a module under STC or field conditions, or in series connection with other modules, as in real operation, or better the yield? Here the awareness of the differences and their meaning is missing. So far, the focus has been on the modules, but the view should go beyond the modules to include external factors, inverters, and the grid. First approaches combine production data with IR-images to consider a longer time period and not just the moment of image recording. The correlation between monitoring data and IR anomalies is not always obvious, but this does not imply that there are no errors or impacts. In the monitoring data, the influences of various system components can overlap and hide module faults.

To prevent misinterpretation of apparent thermal anomalies, meta data (geographical and mechanical site information) and electrical wiring concepts and measurement conditions should be known and involved in the assessment. Two measurements at differing measurement conditions strengthen outcome and failure

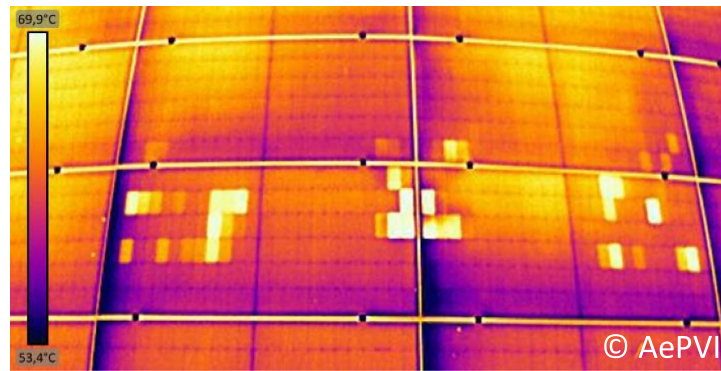


Figure 13. Butterfly architecture modules demonstrating thermal anomalies in both right and left sided areas in IR_{OP} (900 W m^{-2} , $22 \text{ }^\circ\text{C}$ ambient). Butterfly modules features three substrings, but effectively forming two sub-substrings connected in parallel. This electrical connection can lead to thermal anomalies in both substring areas in the forward bias of the diode (active short-circuited or defective short-circuited), although the fault is only present in one sub-substring.

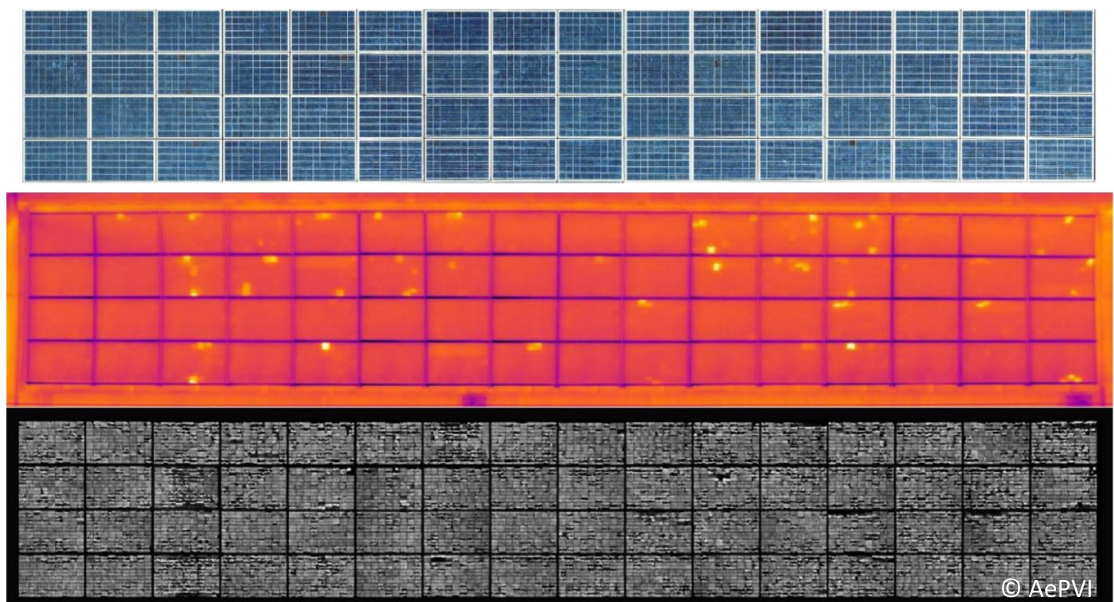


Figure 14. Comparison of visual (top), IR_{OP} (1200 W m^{-2} , $30 \text{ }^\circ\text{C}$ ambient) (center), and EL (bottom) measurements of a roof-top installation [155]. While the EL measurements reveal severe cell damage at almost all modules, only half of the modules show anomalies in IR_{OP} . Because the inverter reacts to the reduced power output of the damaged modules, the operating point shifts to lower power. Then, only the most severely damaged cells show up as thermal anomalies.

analysis of ambiguous images. Promising computer vision tools exist, e.g. [156], what is missing is the implementation for PV. Exemplary results are given by Bommers *et al* [120], if the required datasets exist.

Furthermore, solid and widely accepted criteria for the gravity of thermal anomalies do not exist. There are ambiguous approaches, e.g. suggesting $\Delta T > 20 \text{ K}$ to be severe [136, 157] or projecting power loss to STC conditions. According to our experience the degree of underperformance related to thermal anomalies needs to be evaluated in the context of measurement conditions and additionally the financial backbone and investment concept of the PV power station of interest. Suitable field-relevant metrics should be evaluated and transferred into a standard.

Finally, we strongly recommend a consistent and informative declaration of presented IR-footage including: irradiance, ambient temperature, operating point, and temperature scale (suitable look-up table and color-bar). Furthermore, plant configuration (module type, string layout, inverter type), date, time, a corresponding visual image and wind speed are desirable for a Golden standard. We recommend to use different color-schemes for IR_{OP} , IR_{SC} and IR_{INV} . ML metrics should be enriched with descriptions of the datasets.

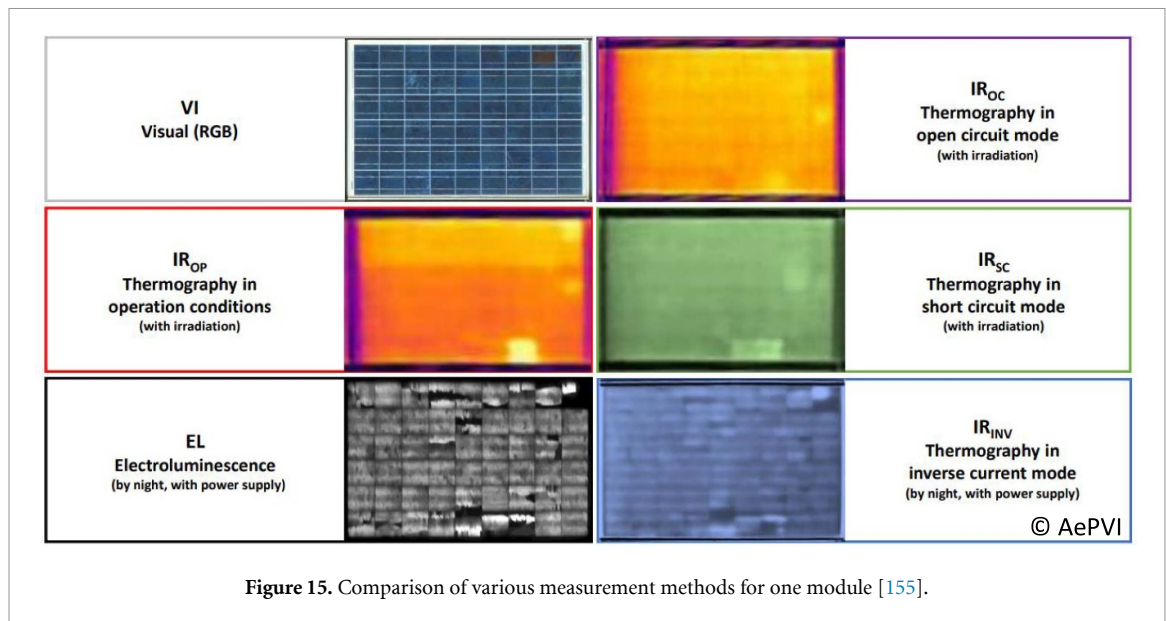


Figure 15. Comparison of various measurement methods for one module [155].

6. Conclusion

The high number of publications in the last years shows that the advantages of thermography, especially quick drone-based IR surveys for troubleshooting PV power stations have been recognized and are being used. To promote the expansion of renewable energy, GWp power stations must be built, operated, and function. These investments must and should deliver electricity for a long time and sustainably. Asset owners, EPCs and O&M companies are interested to achieve a quick and reliable assessment of the status of the PV system, which is actionable. Operation and maintenance are important to ensure that. Solid and reliable bases for decision-making are the prerequisite. Infrared has the potential to become an essential component in the toolbox for inspection and evaluation of GWp PV power stations. For the inspection of these extended PV power stations, the potential of IR imaging cannot yet be fully exploited with current approaches in the field of data acquisition, image processing and assessment.

According to the literature we need more emphasis, a deeper understanding how to quantify the impact of these anomalies on the performance as well as their degradation. Standards and elaborated scientific studies can provide PV stakeholders with the necessary information for actionable O&M. For that suitable datasets of failures plus electrical data need to be generated. Because the failure rates of PV-systems are usually low, less than 8%, it is advantageous to cooperate internationally. Mostly missing are available suitable datasets for adapting, training and test of existing computational instrumentation to PV. Generating these datasets and making them publicly available is the most challenging task. International collaborations on gathering such labeled dataset, following the example of NREL [158], giving access to various datasets. Then, future pipelines of ML tools can capture the entire IR-inspection process steps.

At that, we are convinced that IR-imaging is well equipped for upcoming quality checks of GWp PV power stations.

Data availability statement

All data that support the findings of this study are included within the article (and any supplementary files).

Acknowledgments

This work is supported by the German Federal Ministry for Economic Affairs and Climatic Action (Projects 'COSIMA', FKZ: 0324291A, and 'dig4more', FKZ: 03EE1090B) as well as by the Bavarian State Government (Project 'PVtera—Reliable and cost-efficient photovoltaic power generation on the Terawatt scale,' No. 44-6521a/20/5).

ORCID iD

Claudia Buerhop  <https://orcid.org/0000-0001-5233-6700>

References

- [1] Bloomberg NEF 2022 Solar—10 predictions for 2022 BloombergNEF (available at: [bnef.com](https://www.bnef.com))
- [2] Andrews R 2017 Introduction to aerial inspections *Solarpro* **10** 12–15
- [3] Iliceto A, Previ A, Fleres S and Scuto M 1994 Testing experience of photovoltaic modules for a multimegawatt power plant *Proc. 1994 IEEE 1st World Conf. on Photovoltaic Energy Conversion—WCPEC (A Joint Conf. of PVSC, PVSEC and PSEC)* vol 2 pp 2271–4
- [4] King D L, Kratochvil J A, Quintana M A and McMahon T J 2000 Applications for infrared imaging equipment in photovoltaic cell, module, and system testing *Conf. Record of the 28th IEEE Photovoltaic Specialists Conf.—2000* pp 1487–90
- [5] Bazilian M D, Kamalanathan H and Prasad D K 2002 Thermographic analysis of a building integrated photovoltaic system *Renew. Energy* **26** 449–61
- [6] IEC/TS 62446-3:2017-06 2017 Photovoltaic (PV) systems—requirements for testing, documentation and maintenance, part 3: photovoltaic modules and plants—outdoor infrared thermography *Standard*
- [7] Spagnolo G S, Vecchio P D, Makary G, Papalillo D and Martocchia A 2012 A review of IR thermography applied to PV systems *2012 11th Int. Conf. on Environment and Electrical Engineering* pp 879–84
- [8] Tsanakas J A, Ha L and Buerhop C 2016 Faults and infrared thermographic diagnosis in operating c-Si photovoltaic modules: a review of research and future challenges *Renew. Sustain. Energy Rev.* **62** 695–709
- [9] Gallardo-Saavedra S, Hernández-Callejo L and Duque-Pérez O 2018 Technological review of the instrumentation used in aerial thermographic inspection of photovoltaic plants *Renew. Sustain. Energy Rev.* **93** 566–79
- [10] Rakha T and Gorodetsky A 2018 Review of unmanned aerial system (UAS) applications in the built environment: towards automated building inspection procedures using drones *Autom. Constr.* **93** 252–64
- [11] Jahn U, Herz M, Koentges M, Parlevliet D, Paggi M and Tsanakas I 2018 *Review on Infrared and Electroluminescence Imaging for PV Field Application I.P.T. 13, Subtask 3.3: Report IEA-PVPS T13-10*
- [12] Herraiz Á H, Marugán A P and Márquez F P G 2020 A review on condition monitoring system for solar plants based on thermography *Non-Destructive Testing and Condition Monitoring Techniques for Renewable Energy Industrial Assets* ed M Papaelias, F P G Márquez and A Karyotakis (Boston, MA: Butterworth-Heinemann) ch 7, pp 103–18
- [13] Rahaman S A, Urmee T and Parlevliet D A 2020 PV system defects identification using remotely piloted aircraft (RPA) based infrared (IR) imaging: a review *Sol. Energy* **206** 579–95
- [14] Kandeal A W, Elkadeem M R, Kumar Thakur A, Abdelaziz G B, Sathyamurthy R, Kabeel A E, Yang N and Sharshir S W 2021 Infrared thermography-based condition monitoring of solar photovoltaic systems: a mini review of recent advances *Sol. Energy* **223** 33–43
- [15] Venkatesh S N and Sugumaran V 2021 Fault diagnosis of visual faults in photovoltaic modules: a review *Int. J. Green Energy* **18** 37–50
- [16] He Y, Deng B, Wang H, Cheng L, Zhou K, Cai S and Ciampa F 2021 Infrared machine vision and infrared thermography with deep learning: a review *Infrared Phys. Technol.* **116** 103754
- [17] Najiah Nurul Afifah A, Indrabayu I, Suyuti A and Syafaruddin S A 2021 Review on image processing techniques for damage detection on photovoltaic panels *ICIC International*
- [18] Herrmann W et al 2021 Qualification of photovoltaic (PV) power plants using mobile test equipment *Task 13: Performance, Operation and Reliability of Photovoltaic Systems* ed W Herrmann and U Jahn (IEA PVPS)
- [19] Navid Q, Hassan A, Fardoun A A, Ramzan R and Alraeesi A 2021 Fault diagnostic methodologies for utility-scale photovoltaic power plants: a state of the art review *Sustainability* **13** 1629
- [20] Buerhop C, Schlegel D, Niess M, Vodermayr C, Weißmann R and Brabec C J 2012 Reliability of IR-imaging of PV-plants under operating conditions *Sol. Energy Mater. Sol. Cells* **107** 154–64
- [21] Fernández A, Usamentiaga R, de Arquer P, Fernández M Á, Fernández D, Carús J L and Fernández M 2020 Robust detection, classification and localization of defects in large photovoltaic plants based on unmanned aerial vehicles and infrared thermography *Appl. Sci.* **10** 5948
- [22] Denz J, Hepp J, Buerhop C, Doll B, Hauch J, Brabec C J and Peters I M 2022 Defects and performance of Si PV modules in the field—an analysis *Energy Environ. Sci.* **15** 2180–99
- [23] Haque A, Bharath K V S, Khan M A, Khan I and Jaffery Z A 2019 Fault diagnosis of photovoltaic modules *Energy Sci. Eng.* **7** 622–44
- [24] Köntges M 2014 *Performance and Reliability of Photovoltaic Systems, Subtask 3.2: Review of Failures of Photovoltaic Modules* (IEA, Photovoltaic Power Systems Programme)
- [25] Muehleisen W, Eder G C, Voronko Y, Spielberger M, Sonnleitner H, Knoebel K, Ebner R, Ujvari G and Hirschl C 2018 Outdoor detection and visualization of hailstorm damages of photovoltaic plants *Renew. Energy* **118** 138–45
- [26] Buerhop C, Jahn U, Hoyer U, Lerche B and Wittmann S 2007 Abschlussbericht der Machbarkeitsstudie zur Überprüfung der Qualität von Photovoltaik-Modulen mittels Infrarot-Aufnahmen (available at: www.sev-bayern.de/wp-content/uploads/2018/12/IR-Handbuch.pdf)
- [27] Gulkowski S, Zytowska N, Dragan P, Licholai L, Dębska B, Miąsik P, Szyzka J, Krasoń J and Szalacha A 2018 Temperature distribution analysis of different technologies of PV modules using infrared thermography *E3S Web Conf.* **49** 00044
- [28] Gallardo-Saavedra S, Hernández-Callejo L and Duque-Pérez O 2019 Analysis and characterization of PV module defects by thermographic inspection *Rev. Fac. Ing.—Univ. Ant.* **93** 92–104
- [29] Buerhop-Lutz C, Pickel T, Scheuerpflug H, Camus C, Hauch J and Brabec C J 2017 Statistical analysis of infrared-inspections of PV-plants *33rd EU PVSEC (Amsterdam, The Netherlands)* pp 2320–4
- [30] Weinreich B, Schauer B, Gürzing S and Haas R 2019 Feldstudie 2.0 zur Modul- und Anlagenqualität auf Basis thermographischer Messungen von 1 GW PV-Symp. (Bad Staffelstein)
- [31] García Márquez F P and Segovia Ramírez I 2019 Condition monitoring system for solar power plants with radiometric and thermographic sensors embedded in unmanned aerial vehicles *Measurement* **139** 152–62
- [32] Numan A H, Hussein H A and Dawood Z S 2021 Hot spot analysis of photovoltaic module under partial shading conditions by using IR-imaging technology *Eng. Technol. J.* **39** 1338–44

- [33] Dolara A, Lazaroiu G C and Oglari E 2016 Efficiency analysis of PV power plants shaded by MV overhead lines *Int. J. Energy Environ. Eng.* **7** 115–23
- [34] Cubukcu M and Akanalci A 2020 Real-time inspection and determination methods of faults on photovoltaic power systems by thermal imaging in Turkey *Renew. Energy* **147** 1231–8
- [35] Ebner R, Kubicek B and Újvári G 2013 Non-destructive techniques for quality control of PV modules: infrared thermography, electro- and photoluminescence imaging *IECON 2013–39th Annual Conf. IEEE Industrial Electronics Society* pp 8104–9
- [36] Sinha A, Roy S, Kumar S and Gupta R 2017 Investigation of degradation in photovoltaic modules by infrared and electroluminescence imaging *Advances in Optical Science and Engineering* (Berlin: Springer) pp 3–9
- [37] Gallardo-Saavedra S, Hernández-Callejo L, Alonso-García M, Santos J, Morales-Aragónés J and Alonso-Gómez V 2019 Failure diagnosis on photovoltaic modules using thermography, electroluminescence, RGB and IV techniques *Proc. 36th European Photovoltaic Solar Energy Conf. and Exhibition (Marseille, France)* pp 1171–5
- [38] Koch M, Weber T, Sobottka C, Fladung A, Clemens P and Berghold J 2016 Outdoor electroluminescence imaging of crystalline photovoltaic modules: comparative study between manual ground—level inspections and drone—based aerial surveys *32nd European Photovoltaic Solar Energy Conf. and Exhibition* pp 1736–40
- [39] Doll B, Hepp J, Hoffmann M, Schüler R, Buerhop-Lutz C, Peters I M, Hauch J A, Maier A and Brabec C J 2021 Photoluminescence for defect detection on full-sized photovoltaic modules *IEEE J. Photovolt.* **11** 1419–29
- [40] Mühleisen W et al 2019 Scientific and economic comparison of outdoor characterisation methods for photovoltaic power plants *Renew. Energy* **134** 321–9
- [41] Zefri Y, ElKettani A, SEbari I and ALamallam S A 2018 Thermal infrared and visual inspection of photovoltaic installations by UAV photogrammetry—application case: Morocco *Drones* **2** 41
- [42] Roumpakias E, Bouroutzikas F and Stamatelos A 2016 On-site inspection of PV panels, aided by infrared thermography *Adv. Appl. Sci.* **1** 53–62
- [43] Kumar S, Jena P, Sinha A and Gupta R 2017 Application of infrared thermography for non-destructive inspection of solar photovoltaic module *J. Non-Destr. Test.* **15** 25–32
- [44] Buerhop C, Pickel T, Scheuerpflug H, Dürschner C and Camus C 2016 aIR-PV-check of thin-film PV-plants—detection of PID and other defects in CIGS modules *32nd EU-PVSEC (Munich, Germany)* pp 2021–6
- [45] Lorenzo G D, Araneo R, Mitolo M, Niccolai A and Grimaccia F 2020 Review of O&M practices in PV plants: failures, solutions, remote control, and monitoring tools *IEEE J. Photovolt.* **10** 914–26
- [46] Buerhop C, Scheuerpflug H and Pickel T 2015 Defect analysis of installed PV-modules—IR-thermography and in-string power measurement *31st EU PVSEC (Hamburg, Germany)* pp 1692–7
- [47] Buerhop C and Scheuerpflug H 2014 Comparison of IR-images and module performance under standard and field conditions *29th EU PVSEC (Amsterdam, The Netherlands)* pp 3260–4
- [48] Buerhop C and Scheuerpflug H 2015 Characterization of defects in PV-modules by their temperature development using IR-thermography *31st EU PVSEC (Hamburg, Germany)* pp 1789–92
- [49] Nedelchev I and Zhivomirov H 2020 A combined approach for assessment the functionality of photovoltaic modules in real-world operation *E3S Web of Conf.* (EDP Sciences) p 02006
- [50] Schuss C, Remes K, Leppänen K, Eichberger B and Fabritius T 2021 Thermography of photovoltaic panels and defect detection under outdoor environmental conditions *2021 IEEE Int. Instrumentation and Measurement Technology Conf. (I2MTC)* pp 1–6
- [51] Buerhop-Lutz C, Pickel T, Teubner J, Hauch J and Brabec C J 2019 Analysis of digitized PV-module/system data for failure diagnosis *36th EU-PVSEC (Marseille, France)* pp 1336–41
- [52] Fecher F, Pickel T, Buerhop C, Camus C and Brabec J C 2016 Failure classification of defective PV modules based on maximum power point analysis *32th EU PVSEC (Munich, Germany)* pp 2252–4
- [53] Buerhop C, Fecher F, Dettelbacher J, Pickel T, Camus C, Hauch J and Brabec J C 2016 IR-images of defective PV-modules influenced by short-time changes of the electric system *32nd EU PVSEC (Munich, Germany)* p 2027
- [54] Glavaš H, Žnidarec M, Šljivac D and Veić N 2022 Application of infrared thermography in an adequate reusability analysis of photovoltaic modules affected by hail *Appl. Sci.* **12** 745
- [55] Cardinale-Villalobos L, Rimolo-Donaldio R and Meza C 2020 Solar panel failure detection by infrared UAS digital photogrammetry: a case study *Int. J. Renew. Energy Res.* **10**
- [56] Buerhop C and Scheuerpflug H 2014 Field inspection of PV-modules using aerial, drone-mounted thermography *29th EU-PVSEC (Amsterdam, The Netherlands)* pp 2975–9
- [57] Gallardo-Saavedra S, Hernández-Callejo L and Duque-Perez O 2018 Image resolution influence in aerial thermographic inspections of photovoltaic plants *IEEE Trans. Ind. Inform.* **14** 5678–86
- [58] Sethi R and Kumar P 2017 Advantages and limitations of thermography in utility scale solar PV plants *Conf.: ISES Solar World Conf. 2017 and the IEA SHC Solar Heating and Cooling Conf. for Buildings and Industry 2017* (<https://doi.org/10.18086/SWC.2017.20.09>)
- [59] Hu Y, Cao W, Ma J, Finney S J and Li D 2014 Identifying PV module mismatch faults by a thermography-based temperature distribution analysis *IEEE Trans. Device Mater. Reliab.* **14** 951–60
- [60] Zefri Y, Sebari I, Hajji H and Aniba G 2022 Developing a deep learning-based layer-3 solution for thermal infrared large-scale photovoltaic module inspection from orthorectified big UAV imagery data *Int. J. Appl. Earth Obs. Geoinf.* **106** 102652
- [61] Buerhop-Lutz C, Pickel T, Wenz F, Zetzmann C, Hauch J, Camus C and Brabec C J 2018 Influence of the irradiance on the detection and performance of PID-affected PV-modules *35th EU-PVSEC (Brussels, Belgium)* pp 2001–4
- [62] Buerhop C, Scheuerpflug H and Weißmann R 2011 The role of infrared emissivity of glass on IR-imaging of PV-plants *26th EU-PVSEC (Hamburg, Germany)* pp 3413–6
- [63] Glavaš H, Vukobratović M, Primorac M and Muštran D 2017 Infrared thermography in inspection of photovoltaic panels *2017 Int. Conf. on Smart Systems and Technologies (SST)* pp 63–68
- [64] Breitenstein O and Langenkamp M 2003 *Lock-in Thermography (Advanced Microelectronics)* vol 10 (Berlin: Springer)
- [65] Messwert Emissionsgradtabelle (available at: www.messwert.at/tools/emissionsgradtabelle/)
- [66] Blumm J and Lindemann A 2003/2007 Characterization of the thermophysical properties of molten polymers and liquids using the flash technique *High Temp.—High Press.* **35/36** 627
- [67] Chattopadhyay S et al 2018 Correlating infrared thermography with electrical degradation of PV modules inspected in all-India survey of photovoltaic module reliability 2016 *IEEE J. Photovolt.* **8** 1800–8

- [68] Quater P B, Grimaccia F, Leva S, Mussetta M and Aghaei M 2014 Light unmanned aerial vehicles (UAVs) for cooperative inspection of PV plants *IEEE J. Photovolt.* **4** 1107–13
- [69] Álvarez-Tey G, Jiménez-Castañeda R and Carpio J 2017 Analysis of the configuration and the location of thermographic equipment for the inspection in photovoltaic systems *Infrared Phys. Technol.* **87** 40–46
- [70] Buerhop C, Scheuerpflug H, Pickel T and Camus C 2016 IR-imaging a tracked PV-plant using an unmanned aerial vehicle *32nd EU PVSEC (Munich, Germany)* p 2016
- [71] Henry C, Poudel S, Lee S-W and Jeong H 2020 Automatic detection system of deteriorated PV modules using drone with thermal camera *Appl. Sci.* **10** 3802
- [72] Xi Z, Lou Z, Sun Y, Li X, Yang Q and Yan W 2018 A vision-based inspection strategy for large-scale photovoltaic farms using an autonomous UAV *2018 17th Int. Symp. on Distributed Computing and Applications for Business Engineering and Science (DCABES)* pp 200–3
- [73] Moradi Sizkouhi A M, Esmailifar S M, Aghaei M and Karimkhani M 2022 RoboPV: an integrated software package for autonomous aerial monitoring of large scale PV plants *Energy Convers. Manage.* **254** 115217
- [74] Roggi G, Niccolai A, Grimaccia F and Lovera M 2020 A computer vision line-tracking algorithm for automatic UAV photovoltaic plants monitoring applications *Energies* **13** 838
- [75] Measure Drones in solar (available at: www.measure.com/drones-in-solar-operations) (Accessed 2022)
- [76] McColl D Aerial solar PV inspection 2020 (available at: <http://large.stanford.edu/courses/2020/ph240/mccoll2/>)
- [77] Heliguy 2021 Drones for solar panel inspections
- [78] Oliveira A, Bracht M K, Melo A P, Lamberts R and Rütther R 2021 Evaluation of faults in a photovoltaic power plant using orthomosaics based on aerial infrared thermography *2021 IEEE 48th Photovoltaic Specialists Conf. (PVSC)* pp 2604–10
- [79] Vidal de Oliveira A K, Aghaei M and Ruther R 2019 Automatic fault detection of photovoltaic arrays by convolutional neural networks during aerial infrared thermography *36th EU-PVSEC (Marseille, France)* pp 1302–7
- [80] Uasvision 2016 Drones cut cost of thermographic PV panel inspections (available at: www.uasvision.com/2016/09/15/drones-cut-cost-of-thermographic-pv-panel-inspections/)
- [81] Life td Infrared drone solar inspections (available at: <https://thedronelifej.com/infrared-drone-solar-inspections/>)
- [82] Aghaei M, Madukanya U E, Vidal de Oliveira A K and Rütther R 2018 Fault inspection by aerial infrared thermography in a PV plant after a meteorological tsunami *VII Congresso Brasileiro De Energia Soalr (Granado)*
- [83] Muntwyler U, Schüpbach E and Lanz M Infrared drone for quick and cheap PV inspection *31st EU-PVSEC* pp 1804–6
- [84] Bommes L, Buerhop C, Pickel T, Hauch J, Brabec C J and Peters I M 2022 Georeferencing of photovoltaic modules from aerial infrared videos using structure-from-motion *Prog. Photovolt.* **30** 1122–35
- [85] Kitawa P 2014 Thermografie an photovoltaikanlagen (available at: <https://kitawa.de/thermografie-pv-anlagen>)
- [86] Andrews R 2018 Aerial inspections (Solarplaza) white paper
- [87] Raptormaps Available levels of inspection (available at: <https://raptormaps.com/turnkey-services/>) (Accessed 2022)
- [88] Solarif Aircraft inspection (available at: www.solarif.com/drone-inspection-2/) (Accessed 2022)
- [89] Raptormaps 2021 Guide to solar PV inspection via manned aircraft (available at: <https://f.hubspotusercontent40.net/hubfs/3446343/2021%20Guide%20to%20Manned%20Aircraft%20PV%20Inspections.pdf>)
- [90] Andrews R 2018 Identifying and addressing underperforming solar assets *Solarpro* **11** 12–18
- [91] Grimaccia F, Leva S and Niccolai A 2017 PV plant digital mapping for modules' defects detection by unmanned aerial vehicles *IET Renew. Power Gener.* **11** 1221–8
- [92] Francesco G, Sonia L and Alessandro N 2018 A semi-automated method for defect identification in large photovoltaic power plants using unmanned aerial vehicles *2018 IEEE Power & Energy Society General Meeting (PESGM)* (IEEE) pp 1–5
- [93] Dotenco S, Dalsass M, Winkler L, Würzner T, Brabec C, Maier A and Gallwitz F 2016 Automatic detection and analysis of photovoltaic modules in aerial infrared imagery *2016 IEEE Winter Conf. on Applications of Computer Vision (WACV)* (Lake Placid, NY: IEEE) pp 1–9
- [94] Niccolai A, Grimaccia F and Leva S 2019 Advanced asset management tools in photovoltaic plant monitoring: UAV-based digital mapping *Energies* **12** 4736
- [95] Kim D, Youn J and Kim C 2016 Automatic photovoltaic panel area extraction from UAV thermal infrared images *J. Korean Soc. Surv. Geod. Photogramm. Cartogr.* **34** 559–68
- [96] Kim D, Youn J and Kim C 2017 Automatic fault recognition of photovoltaic modules based on statistical analysis of UAV thermography *Int. Arch. Photogramm. Remote Sens. Spat. Inf. Sci.* **42** 179
- [97] Wang Q, Paynabar K and Pacella M 2021 Online automatic anomaly detection for photovoltaic systems using thermography imaging and low rank matrix decomposition *J. Qual. Technol.* **1**–14
- [98] Aghaei M, Leva S and Grimaccia F 2016 PV power plant inspection by image mosaicing techniques for IR real-time images *2016 IEEE 43rd Photovoltaic Specialists Conf. (PVSC)* (IEEE) pp 3100–5
- [99] Wu F, Zhang D, Li X, Luo X, Wang J, Yan W, Chen Z and Yang Q 2017 Aerial image recognition and matching for inspection of large-scale photovoltaic farms *2017 Int. Smart Cities Conf. (ISC2)* (IEEE) pp 1–6
- [100] Carletti V, Greco A, Saggese A and Vento M 2020 An intelligent flying system for automatic detection of faults in photovoltaic plants *J. Ambient Intell. Humaniz. Comput.* **11** 2027–40
- [101] Tsanakas J A, Chrysostomou D, Botsaris P N and Gasteratos E A 2013 Fault diagnosis of photovoltaic modules through image processing and Canny edge detection on field thermographic measurements *Int. J. Sustain. Energy* **34** 351–72
- [102] Arenella A, Greco A, Saggese A and Vento M 2017 Real time fault detection in photovoltaic cells by cameras on drones *Int. Conf. Image Analysis and Recognition* (Springer) pp 617–25
- [103] Addabbo P, Angrisano A, Bernardi M L, Gagliarde G, Mennella A, Nisi M and Ullo S L 2018 UAV system for photovoltaic plant inspection *IEEE Aerosp. Electron. Syst. Mag.* **33** 58–67
- [104] Jeong H, Kwon G-R and Lee S-W 2020 Deterioration diagnosis of solar module using thermal and visible image processing *Energies* **13** 2856
- [105] Zhang H, Hong X, Zhou S and Wang Q 2019 Infrared image segmentation for photovoltaic panels based on Res-UNet *Chinese Conf. on Pattern Recognition and Computer Vision (PRCV)* (Springer) pp 611–22
- [106] Greco A, Pironti C, Saggese A, Vento M and Vigilante V 2020 A deep learning based approach for detecting panels in photovoltaic plants *Proc. 3rd Int. Conf. on Applications of Intelligent Systems* pp 1–7
- [107] Vega Díaz J J, Vlaminck M, Lefkaditis D, Orjuela Vargas S A and Luong H 2020 Solar panel detection within complex backgrounds using thermal images acquired by UAVs *Sensors* **20** 6219

- [108] Bommers L, Pickel T, Buerhop C, Brabec C J and Peters I M 2021 Computer vision tool for detection, mapping and fault classification of PV modules in aerial IR videos *Prog. Photovolt.* **29** 1236–51
- [109] Aghaei M, Grimaccia F, Gonano C A and Leva S 2015 Innovative automated control system for PV fields inspection and remote control *IEEE Trans. Ind. Electron.* **62** 7287–96
- [110] Et-taleby A, Boussetta M, Benslimane M and Khadka D B 2020 Faults detection for photovoltaic field based on K-means, elbow, and average silhouette techniques through the segmentation of a thermal image *Int. J. Photoenergy* **2020** 6617597
- [111] Jaffery Z A, Dubey A K, Haque I and Haque A 2017 Scheme for predictive fault diagnosis in photo-voltaic modules using thermal imaging *Infrared Phys. Technol.* **83** 182–7
- [112] Ali M U, Saleem S, Masood H, Kallu K D, Masud M, Alvi M J and Zafar A 2022 Early hotspot detection in photovoltaic modules using color image descriptors: an infrared thermography study *Int. J. Energy Res.* **46** 774–85
- [113] Alsafasfeh M, Abdel-Qader I, Bazuin B, Alsafasfeh Q and Su W 2018 Unsupervised fault detection and analysis for large photovoltaic systems using drones and machine vision *Energies* **11** 2252
- [114] Niazi K A K, Akhtar W, Khan H A, Yang Y and Athar S 2019 Hotspot diagnosis for solar photovoltaic modules using a Naive Bayes classifier *Sol. Energy* **190** 34–43
- [115] Vlaminck M, Heimbuchel R, Philips W and Luong H 2022 Region-based CNN for anomaly detection in PV power plants using aerial imagery *Sensors* **22** 1244
- [116] Dunderdale C, Bretteny W, Clohessy C and van Dyk E E 2020 Photovoltaic defect classification through thermal infrared imaging using a machine learning approach *Prog. Photovolt., Res. Appl.* **28** 177–88
- [117] Manno D, Cipriani G, Ciulla G, di Dio V, Guarino S and Lo Brano V 2021 Deep learning strategies for automatic fault diagnosis in photovoltaic systems by thermographic images *Energy Convers. Manage.* **241** 114315
- [118] Segovia Ramírez I, Das B and García Márquez F P 2022 Fault detection and diagnosis in photovoltaic panels by radiometric sensors embedded in unmanned aerial vehicles *Prog. Photovolt., Res. Appl.* **30** 240–56
- [119] Su Y, Tao F, Jin J and Zhang C 2021 Automated overheated region object detection of photovoltaic module with thermography image *IEEE J. Photovolt.* **11** 535–44
- [120] Bommers L, Hoffmann M, Buerhop C, Hauch J, Brabec C J and Peters I M 2022 Anomaly detection in IR images of PV modules using supervised contrastive learning *Prog. Photovolt.* **30** 597–614
- [121] Lee D H and Park J H 2019 Developing inspection methodology of solar energy plants by thermal infrared sensor on board unmanned aerial vehicles *Energies* **12** 2928
- [122] Tsanakas J A, Ha L D and Al Shakarchi F 2017 Advanced inspection of photovoltaic installations by aerial triangulation and terrestrial georeferencing of thermal/visual imagery *Renew. Energy* **102** 224–33
- [123] Nisi M, Menichetti F, Muhammad B, Prasad R, Cianca E, Mennella A, Gagliardi G and Marenchino D 2016 EGNSS high accuracy system improving photovoltaic plant maintenance using RPAS integrated with low-cost RTK receiver *Proc. Global Wireless Summit Conf.*
- [124] Alonso-García M C, Ruiz J M and Chenlo F 2006 Experimental study of mismatch and shading effects in the I–V characteristic of a photovoltaic module *Sol. Energy Mater. Sol. Cells* **90** 329–40
- [125] Catalano A P, Scognamillo C, Guerriero P, Daliendo S and d'Alessandro V 2021 Using EMPHASIS for the thermography-based fault detection in photovoltaic plants *Energies* **14** 1559
- [126] Kauppinen T, Panouillot P-E, Siikanen S, Athanasakou E, Baltas P and Nikopoulous B 2015 About infrared scanning of photovoltaic solar plant *Proc. SPIE* **9485** 948517
- [127] Andrews R 2022 Impact of climate on thermally-detectable module degradation modes *NREL Photovoltaic Reliability Workshop (Denver, CO)*
- [128] Vergura S and Marino F 2017 Quantitative and computer-aided thermography-based diagnostics for PV devices: part I—framework *IEEE J. Photovolt.* **7** 822–7
- [129] Teubner J, Buerhop-Lutz C, Pickel T, Hauch J, Camus C J and Brabec C J 2019 Quantitative assessment of the power loss of silicon PV modules by IR thermography and its dependence on data filtering criteria *Prog. Photovolt.* **27** 479
- [130] Denz J, Buerhop-Lutz C, Pickel T, Hauch J, Camus C and Brabec C J 2020 Quantitative assessment of the power loss of silicon PV modules by IR thermography and its practical application in the field *37th EU-PVSEC (Lisboan, Portugal)* pp 1542–7
- [131] Martínez-Moreno F, Figueiredo G and Lorenzo E 2018 In-the-field PID related experiences *Sol. Energy Mater. Sol. Cells* **174** 485–93
- [132] Buerhop-Lutz C, Fecher F W, Pickel T, Patel T, Zetzmann C, Camus C, Hauch J and Brabec C J 2017 Impact of PID on industrial roof-top PV-installations *Proc. SPIE* **10370** 103700B
- [133] Buerhop C, Pickel T, Blumberg T, Adams J, Wrana S, Dalsass M, Camus C, Zetzmann C, Hauch J and Brabec C J 2016 Correlation of potential induced degradation (PID) in PV-modules with monitored string power output *Proc. SPIE* **9938** 99380J
- [134] van der Vaeren S 2018 The have-it-all synergy between monitoring & aerial data for solar PV (available at: www.PESSOLAR.com)
- [135] Teubner J, Kruse I, Scheuerpflug H, Buerhop-Lutz C, Hauch J, Camus C and Brabec C J 2017 Comparison of drone-based IR-imaging with module resolved monitoring power data *7th Int. Conf. on Silicon Photovoltaics, Silicon PV 2017 (Freiburg, Germany)*
- [136] Moretón R, Lorenzo E and Narvarte L 2015 Experimental observations on hot-spots and derived acceptance/rejection criteria *Sol. Energy* **118** 28–40
- [137] Winston D P 2019 Efficient output power enhancement and protection technique for hot spotted solar photovoltaic modules *IEEE Trans. Device Mater. Reliab.* **19** 664–70
- [138] Ma M, Liu H, Zhang Z, Yun P and Liu F 2019 Rapid diagnosis of hot spot failure of crystalline silicon PV module based on I–V curve *Microelectron. Reliab.* **100–1** 113402
- [139] Čabo F G, Marinić-Kragić I, Garma T and Nižetić S 2021 Development of thermo-electrical model of photovoltaic panel under hot-spot conditions with experimental validation *Energy* **230** 120785
- [140] Muñoz J, Lorenzo E, Martínez-Moreno F, Marroyo L and García M 2008 An investigation into hot-spots in two large grid-connected PV plants *Prog. Photovolt., Res. Appl.* **16** 693–701
- [141] Islam M, Hasan G, Ahmed I, Amin M, Dewan S and Rahman M M 2019 Infrared thermography based performance analysis of photovoltaic modules *2019 Int. Conf. on Energy and Power Engineering (ICEPE)* pp 1–5
- [142] Muttillio M, Nardi I, Stornelli V, de Rubeis T, Pasqualoni G and Ambrosini D 2020 On field infrared thermography sensing for PV system efficiency assessment: results and comparison with electrical models *Sensors* **20** 1055

- [143] Pinceti P, Profumo P, Travaini E and Vanti M 2019 Using drone-supported thermal imaging for calculating the efficiency of a PV plant 2019 *IEEE Int. Conf. on Environment and Electrical Engineering and 2019 IEEE Industrial and Commercial Power Systems Europe (EEEIC/I&CPS Europe)* pp 1–6
- [144] Buerhop-Lutz C, Fecher F, Pickel T, Häring A, Adamski T, Camus C, Hauch J and Brabec C J 2018 Verifying defective PV-module recognition by IR-imaging and module optimizers *Prog. Photovolt.* **26** 622–30
- [145] Dalsass M, Scheuerpflug H, Fecher F, Buerhop C, Camus C and Brabec C J 2016 Correlation between the generated string powers of a photovoltaic power plant and module defects detected by aerial thermography *IEEE PVSC 43rd (Portland, USA)* pp 3113–8
- [146] Dalsass M, Scheuerpflug H, Maier M and Brabec C J 2015 Correlation between the monitoring data of a photovoltaic power plant and module defects detected by drone-mounted thermography *31st EU-PVSEC (Hamburg, Germany)* pp 1793–8
- [147] Stegner C, Dalsass M, Luchscheider P and Brabec C J 2018 Monitoring and assessment of PV generation based on a combination of smart metering and thermographic measurement *Sol. Energy* **163** 16–24
- [148] Skomedal Å F, Aarseth B L, Haug H, Selj J and Marstein E S 2020 How much power is lost in a hot-spot? A case study quantifying the effect of thermal anomalies in two utility scale PV power plants *Sol. Energy* **211** 1255–62
- [149] Aarseth B L, Skomedal A, Ogaard M B and Marstein E S 2020 The influence of thermal signatures observed with infrared thermography on power production in a utility scale power plant *Proc. 37th European Photovoltaic Solar Energy Conf.* pp 1360–3
- [150] Skomedal Å F, Ogaard M B, Haug H and Marstein E S 2021 Robust and fast detection of small power losses in large-scale PV systems *IEEE J. Photovolt.* **11** 819–26
- [151] Aarseth B L and Marstein E S 2019 Defect recognition and power loss estimation using infrared thermography *Proc. European Photovoltaic Solar Energy Conf.* pp 1563–8
- [152] Dalsass M, Schmitt P, Buerhop C, Luchscheider P, Hauch J A, Brabec J and Camus C J 2018 Utilization of inverter operation point shifts as a quality assessment tool for photovoltaic systems *IEEE J. Photovolt.* **8** 315–21
- [153] NASA 2021 Taking flight on another world
- [154] BMWi 2020 im humanitären Einsatz—transport von Medikamenten ... mit Drohnen *Unbemanntes Fliegen im Dienst von Mensch, Natur und Gesellschaft*
- [155] Fladung A and Schlipf J 2021 Aerial PV inspection
- [156] Lowin M, Kellner D, Kohl T and Mihale-Wilson C 2021 From physical to virtual: leveraging drone imagery to automate photovoltaic system maintenance *INFORMATIK 2021*
- [157] Libra M, Daneczek M, Leseticky J, Poulek V, Sedláček J and Beranek V 2019 Monitoring of defects of a photovoltaic power plant using a drone *Energies* **12** 795
- [158] NREL 2022 Developer network (available at: <https://developer.nrel.gov/docs/solar/pvdaq-v3/>)